THE OPEN BOOK SERIES 5

Gauge Theory and Low-Dimensional Topology: Progress and Interaction

Lifting Lagrangian immersions in $\mathbb{C}P^{n-1}$ to Lagrangian cones in $\mathbb{C}^n$

Scott Baldridge, Ben McCarty and David Vela-Vick

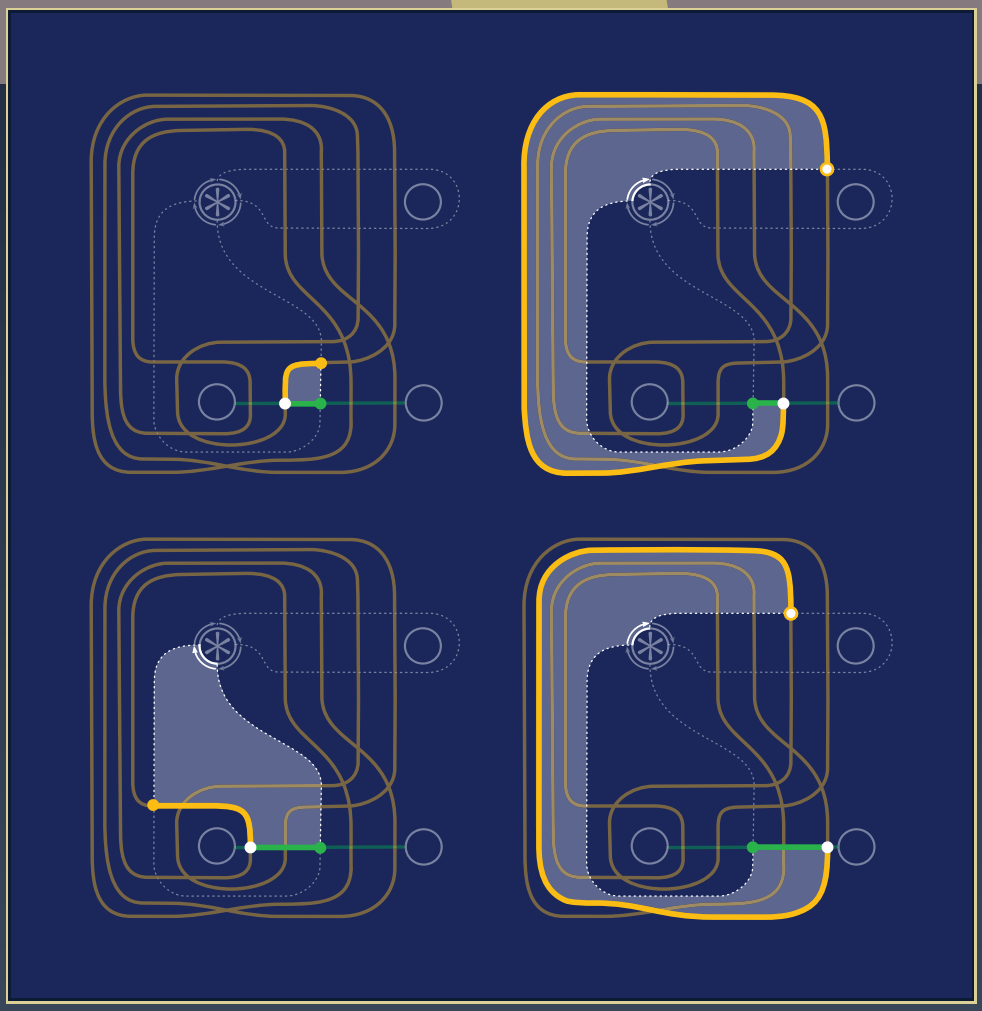

msp

THE OPEN BOOK SERIES **5** (2022)
Gauge theory and low-dimensional topology: progress and interaction
https://doi.org/10.2140/obs.2022.5.43

msp

Lifting Lagrangian immersions in $\mathbb{C}P^{n-1}$ to Lagrangian cones in $\mathbb{C}^n$

Scott Baldridge, Ben McCarty and David Vela-Vick

We show how to lift Lagrangian immersions in $\mathbb{C}P^{n-1}$ to produce Lagrangian cones in $\mathbb{C}^n$, and use this process to produce several families of examples of Lagrangian cones and special Lagrangian cones. As an application of this theorem, for $n = 3$ we show how to produce Lagrangian cones that are isotopic to the Harvey–Lawson special Lagrangian cone and the trivial cone. The projections of the Legendrian links of both of these cones to $\mathbb{C}P^2$ are immersions with four and seven transverse double points. We expect that these double points represent the chord generators of the 0-filtration level of a suitably defined version of Legendrian contact homology of the links.

1. Introduction

This paper focuses on creating models for Lagrangian cones. The motivation for this paper arises from the string theory model in physics. According to the theory, our universe consists of the standard Minkowski space-time, $\mathbb{R}^4$, together with a complex Calabi–Yau 3-fold, X. Based upon physical grounds, the SYZ-conjecture of Strominger, Yau, and Zaslow [32] expects that this Calabi–Yau manifold can be viewed as a fibration by 3-tori with some singular fibers. These singular fibers are not well understood. The standard approach is to model them locally as special Lagrangian cones $C \subset \mathbb{C}^3$ (by cone, we mean a subset $C \subset \mathbb{C}^3$ such that $r \cdot C = C$ for any real number $r > 0$). Such a cone can be characterized by its link, $C \cap S^5$, which is a Legendrian surface.

Special Lagrangian cones in $\mathbb{C}^3$ are solutions to nonlinear degree 2 and 3 partial differential equations. Many papers on the subject to date have used this perspective, often by using examples from algebraic geometry. However, given that the cone

MSC2020: 53D17, 53D35, 57R17.
Keywords: lagrangian, cone, SYZ, Calabi–Yau, knot, Harvey–Lawson, hypercube diagram, grid diagram, contact homology.

can be characterized by the Legendrian link, this topic is very closely related to the study of knotted Legendrian submanifolds. This relationship connects it to a great deal of work in the area of contact topology. In this area much progress has been made, at least in part, due to the fact that there are topological and combinatorial representations of such submanifolds. In dimension 3, where the problem of understanding Legendrian submanifolds amounts to classifying Legendrian knots up to isotopy, such diagrammatic representations are easy to generate. For instance, grid diagrams can be used to obtain combinatorial representations of both front and Lagrangian projections of Legendrian knots (see [4; 5; 7; 19; 28]). In higher dimensions, there are fewer such constructions. In [9], Ekholm, Etnyre, and Sullivan present front spinning as a way of constructing one class of knotted Legendrian tori, showing that the theory of Legendrian submanifolds of $\mathbb{R}^{2n+1}$ is at least as rich in higher dimensions as it is in dimension 3. To accomplish this, they extend the definition of Legendrian contact homology to $\mathbb{R}^{2n+1}$. In [4], it was shown that knotted Legendrian tori could be constructed from Lagrangian hypercube diagrams, and it was shown how to compute several invariants from such a diagram. In [16], Lambert-Cole showed how to generalize that construction to produce a product operation on Legendrian submanifolds.

1A. ***Lifts of Lagrangian immersions in $\mathbb{C}P^{n-1}$ to S^{2n-1}.*** With the appropriate setup, it is possible to construct models of Legendrian surfaces in S^5 so that the resulting cone in $\mathbb{C}^3$ is Lagrangian, and in some cases, special Lagrangian. The lifting theorem describes precisely the conditions under which an immersion into $\mathbb{C}P^{n-1}$ lifts to an embedded Legendrian submanifold of S^{2n-1} that gives rise to a Lagrangian cone.

Lifting theorem. *Let Σ be a closed, connected, smooth $(n-1)$-manifold, and $f : \Sigma \to \mathbb{C}P^{n-1}$ be a Lagrangian immersion with respect to the integral Fubini–Study symplectic form $\frac{1}{\pi}\omega_{FS}$. Let $\pi : S^{2n-1} \to \mathbb{C}P^{n-1}$ be the principle Hopf S^1-bundle with connection 1-form $\frac{i}{\pi}\alpha$ where $\alpha = i_0^*\big(\frac{1}{2}\sum_{i=1}^n x_i dy_i - y_i dx_i\big)$ for the identity map $i_0 : S^{2n-1} \to \mathbb{C}^n$. For each chart $\Psi_j : B_j \times S^1 \to S^{2n-1}$ (see Section 4), there exists a 1-form τ_j such that $\Psi_j^*(\alpha) = \frac{1}{2}(dt - \tau_j)$ where $\tau_j = -\sum_{i=1,\, i\neq j}^n (x_i dy_i - y_i dx_i)$.*
If

(1) $\Gamma \int_\gamma \tau = 0 \bmod 2\pi$ *for all* $[\gamma] \in H_1(\Sigma; \mathbb{Z})$, *and*

(2) *for all distinct points $x_1, \ldots, x_k \in \Sigma$ such that $f(x_1) = f(x_j)$ for all $j \leq k$, and a choice of path γ_j from x_1 to x_j in Σ for $2 \leq j \leq k$, the set*

$$\left\{ \left(\Gamma \int_{f(\gamma_j)} \tau \right) \bmod 2\pi \;\middle|\; 2 \leq j \leq k \right\}$$

has $k-1$ distinct values, none of which are equal to 0,

then $f : \Sigma \to \mathbb{C}P^{n-1}$ lifts to an embedding $\tilde{f} : \Sigma \to S^{2n-1}$ such that the image (the lift) $\widetilde{\Sigma}$ is a Legendrian submanifold of (S^{2n-1}, α). In turn, the cone $c\widetilde{\Sigma}$ is Lagrangian in $\mathbb{C}^n$ with respect to the standard symplectic structure $\omega_0 = \sum_{i=1}^{n} dx_i \wedge dy_i$.

Remark 1.1. The 1-form τ_j may be thought of as a multiple of a contact form on S^{2n-1} as observed in Section 4.

Remark 1.2. The integral $\Gamma \int_\gamma$ refers to a *lifting integral* (see Definition 4.8).

Remark 1.3. The second condition of the lifting theorem is stated for multiple points in general, but in most examples, we will only be working with double points or S^1-families of double points.

1B. ***Legendrian contact homology and Lagrangian cones.*** While the lifting theorem is quite general, it is often possible (and simpler) to work within a single chart of $\mathbb{C}P^{n-1}$. To construct a local model for special Lagrangian cones, we work in the symplectic manifold $(\mathbb{C}^n, \omega, \Omega)$ where $\mathbb{C}^n$ has complex coordinates $(z_1, \ldots, z_n)$, $\omega_0 = \frac{i}{2}(dz_1 \wedge d\overline{z_1} + \cdots + dz_n \wedge d\overline{z_n})$ is the standard Kähler form, and $\Omega = dz_1 \wedge \cdots \wedge dz_n$ is the holomorphic volume form (see [14]).

Definition 1.4. A cone $C \subset \mathbb{C}^n$ is special Lagrangian if it is Lagrangian and $\operatorname{Im} \Omega|_C \equiv 0$ or, equivalently, if C is calibrated (in the sense of [13]) with respect to $\operatorname{Re} \Omega$.

As a first step, we will focus first on the construction of Lagrangian cones. Observe that the kernel of the 1-form

$$\alpha = \tfrac{1}{2}(x_1 dy_1 - y_1 dx_1 + \cdots + x_n dy_n - y_n dx_n),$$

where $z_j = x_j + iy_j$, restricted to the unit sphere, generates the standard contact structure for S^{2n-1} and that $\alpha = \iota_R \omega$, where $R = 2\big(\sum_{i=1}^{n} x_i \frac{\partial}{\partial x_i} + y_i \frac{\partial}{\partial y_i}\big)$. This means that, given a Legendrian submanifold $\Sigma \subset S^{2n-1}$, the associated cone $c\Sigma$, obtained by scaling Σ by positive real numbers, is automatically Lagrangian. Moreover, any Lagrangian cone with vertex at the origin, must intersect S^{2n-1} in a Legendrian surface. Hence, with respect to the standard contact structure on S^{2n-1} and the standard symplectic form on $\mathbb{C}^n$, a given submanifold of $S^{2n-1} \subset \mathbb{C}^n$ is Legendrian if and only the associated cone in $\mathbb{C}^n$ is Lagrangian.

In knot theory, the trivial knot and the trefoil are the two simplest types of knots. Analogously, we use the lifting theorem in this paper to study the two simplest Lagrangian cones: the trivial cone and the Harvey–Lawson special Lagrangian cones. We begin by recalling the construction of the Harvey–Lawson special Lagrangian cone.

Example 1.5. Example III.3.A in [13] introduced one of the first nontrivial families of examples of special Lagrangian cones, collectively known as *the Harvey–Lawson*

cone. In particular, they proved that the cone on the $(n-1)$-tori defined by the following two sets is a special Lagrangian cone:

$$T^+ = \{(e^{i\theta_1}, \dots, e^{i\theta_n}) \in \mathbb{C}^n \mid \theta_1 + \cdots + \theta_n = 0\},$$
$$T^- = \{(e^{i\theta_1}, \dots, e^{i\theta_n}) \in \mathbb{C}^n \mid \theta_1 + \cdots + \theta_n = \pi\}.$$

Observe that we may rewrite T^+ as

$$T^+ = \{(e^{i\theta_1}, \dots, e^{i\theta_{n-1}}, e^{-i(\theta_1+\cdots+\theta_{n-1})}) \mid \theta_1, \dots, \theta_{n-1} \in S^1\}, \tag{1-1}$$

and we will call the cone on T^+ the *Harvey–Lawson cone.*

In [30], Sabloff used combinatorial methods to define a version of Legendrian contact homology for Legendrian knots in circle bundles over Riemann surfaces. We expect that similar methods give rise to a version of Legendrian contact homology in the present context as well. Sabloff's Legendrian contact homology is filtered by the "winding number" of the Reeb chord around the fiber. As such, the short Reeb chords in the 0-filtration level (i.e., those that do not wrap around the fiber) are crucial to any calculation of the homology. In this context, as an application of the lifting theorem we calculate the expected generators of the 0-filtration level of the Legendrian contact homology of the torus given by the intersection of the Harvey–Lawson special Lagrangian cone with S^5 using the standard contact structure α.

Theorem 3.16. *Let $T^2 \subset S^5$ be the torus constructed in Example 3.1, which is Legendrian isotopic to $T^+ \subset S^5$. Then the* 0*-filtration level of the Legendrian contact homology of T^2 is generated by four pairs of short Reeb chords, two each in gradings* 4, 6, 7, *and* 9. *These Reeb chords correspond to the double points of T^2 via the projection of T^2 under $\pi : S^5 \to \mathbb{C}P^2$ (as described in Example 3.1).*

Many of the technical calculations in this paper are devoted to proving this theorem (and Theorem 5.3). The Harvey–Lawson special Lagrangian cone has an associated Legendrian torus in S^5 that is a 3-fold cover of a (standard) Lagrangian torus in $\mathbb{C}P^2$. The isotopies that are used to place this Legendrian torus in general position are delicate and have to be done in steps: first we find projections with double point circles, and then we perturb the resulting surface to obtain one whose projection to $\mathbb{C}P^{n-1}$ has isolated transverse double points. It is only in this carefully orchestrated setup that we can count the double points, and hence the filtration level 0 generators of contact homology. We use a similar approach in Sections 3C and 3D to construct examples of Lagrangian cones arising from products of Legendrian knots.

Example 1.6. The trivial cone is simply a Lagrangian copy of $\mathbb{R}^n \subset \mathbb{C}^n$. In particular, the following is well known and easy to check:

Theorem 1.7. *If $f : \mathbb{R}^n \to \mathbb{C}^n$ is given by $(x_1, \dots, x_n) \mapsto (x_1\eta_1, \dots, x_n\eta_n)$, where $\eta = (\eta_1, \dots, \eta_n)$ is a complex vector with $\eta_j \neq 0$ for all j, then the image of f is Lagrangian with respect to the standard symplectic form ω.*

For some choices of η the trivial cone is special Lagrangian. For example, when $n = 3$ a direct calculation shows that for $\eta = (a_1 + ib_1, a_2 + ib_2, a_3 + ib_3)$, if

$$a_2a_3b_1 + a_1a_3b_2 + a_1a_2b_3 - b_1b_2b_3 = 0$$

then the map $f : \mathbb{R}^3 \to \mathbb{C}^3$ given by

$$(x_1, \dots, x_n) \mapsto (x_1(a_1 + ib_1), x_2(a_2 + ib_2), x_3(a_3 + ib_3))$$

is a special Lagrangian cone.

While the cone is just a copy of $\mathbb{R}^3 \subset \mathbb{C}^3$, its intersection with $S^5 \subset \mathbb{C}^3$ is a copy of S^2 that double covers a copy of $\mathbb{R}P^2$ under the projection $\pi : S^5 \to \mathbb{C}P^2$. For computations of Legendrian contact homology, it is desirable to perturb the cone so that, in the projection, we see only isolated transverse double points. Unlike with the Harvey–Lawson cone, whose link embeds in a single chart (see Section 2), the lift of $\mathbb{R}P^2$ used to study the trivial cone requires the full strength of the lifting theorem.

As with the Harvey–Lawson cone, we use the lifting theorem to obtain a similar theorem about the expected generators of the trivial cone's Legendrian contact homology.

Theorem 5.3. *Let $S \subset S^5$ be the Legendrian 2-sphere obtained from intersecting the trivial cone with S^5 and then perturbing it via Legendrian isotopy to one with transverse double points (see Section 5). Then the 0-filtration level of the Legendrian contact homology of S is generated by 7 pairs of short Reeb chords. These Reeb chords correspond to the double points of the projection of S under $\pi : S^5 \to \mathbb{C}P^2$.*

1C. ***Lagrangian cones given by knot diagrams.*** In [4], pairs of grid diagrams for knots were used to construct immersed Lagrangian tori in $\mathbb{R}^4$, whose lifts to $\mathbb{R}^5$ equipped with the standard contact structure are embedded Legendrian tori. In Sections 3C and 3D, we show how to adapt this construction to produce Legendrian tori in S^5 whose associated cones in $\mathbb{C}^3$ are Lagrangian. This allows us to construct infinite families of Lagrangian cones, some of which may be isotopic to special Lagrangian cones. Future research will explore the question of under what conditions this happens.

1D. ***Outline.*** The remainder of the paper is organized as follows. In Section 2, we discuss the background information leading to the statement of a useful simplification of the lifting theorem (cf. Theorem 2.2), and various examples we can construct using it. In Section 4, we prove the lifting theorem, and in Section 5 we give an example of a lift using it. Section 6 explores the implications of the lifting theorem

for the study of Legendrian submanifolds of S^{2n-1}. Finally, Section 7 introduces some questions regarding the study of Hamiltonian minimal submanifolds using the theorems and examples in this paper.

2. Lifting theorem in a single chart

In this section we develop a special case of the lifting theorem that we use for constructing examples of embedded Legendrian submanifolds of S^{2n-1} as lifts of Lagrangian immersions in $\mathbb{C}P^{n-1}$.

The local theory for lifting Lagrangian immersions into a symplectic manifold to some S^1-bundle over that manifold comes out of the theory of fiber bundles. Given a $2n$-dimensional symplectic manifold (X^{2n}, ω) with an integral symplectic form, let $\pi : L \to X^n$ be the complex line bundle such that $c_1(L) = [\omega]$. By the theory of line bundles (see [12]), we know that there is a 1-form η on the unit circle bundle $P = U(L)$ such that $d\eta = \pi^*(\omega)$. In this case, $i\eta \in \Omega^1(P; i\mathbb{R})$ is called the connection 1-form. If $f : \Sigma^n \to X^{2n}$ is a Lagrangian immersion of a connected n-dimensional manifold Σ, then $[f(\Sigma^n)] \cap [\omega] = 0$ and the pull-back of the S^1-bundle P over Σ is trivial. Given

$$\begin{array}{ccc} f^*(P) & \xrightarrow{F} & P \\ \downarrow & & \downarrow \pi \\ \Sigma & \xrightarrow{f} & X^{2n} \end{array}$$

then $f^*(P) \cong \Sigma \times S^1$. In turn, there exists a section $\sigma : \Sigma \to f^*(P)$ which gives an immersed submanifold $F(\sigma(\Sigma))$ of P (see [34]).

In this setup, η is a contact form for P. In general, $F(\sigma(\Sigma))$ will not be Legendrian with respect to η. However, we can always use η to lift a neighborhood U of $x_0 \in \Sigma$ to a Legendrian submanifold of P as follows: using the diffeomorphism $f^*(P) \cong \Sigma \times S^1$ along with the section $\sigma(x) = (x, 1)$, we can define a trivialization of $P|_U$ by (x, e^{it}) for $x \in U$ and $t \in \mathbb{R}$. For $x \in U$, let γ be a path in U from $\gamma(0) = x_0$ to $\gamma(1) = x_1$. This path gives rise to a path Γ in $P|_U$ using the holonomy of the connection 1-form $F^*(\eta)$. That is, Γ is the unique path such that $\Gamma(0) = (x_0, 1)$, $\pi(\Gamma(s)) = \gamma(s)$, and $F^*(\eta)(\Gamma'(s)) = 0$ for all $s \in (0, 1)$. Define the lift $\tilde{f} : U \to P$ by $\tilde{f}(x) = F(\Gamma(1))$.

This map is independent of the path chosen in the contractible neighborhood U because f is a Lagrangian immersion (the restricted holonomy group at x_0 is trivial).

We can write this holonomy map down explicitly in terms of $\Sigma \times S^1$ and the section σ given by coordinates (x, e^{it}) where $x \in \Sigma$ and $t \in \mathbb{R}$. Suppose

$$F^*(\eta) = k(dt - \tau),$$

where $k \in \mathbb{R}$ is a constant, and $\tau \in \Omega^1(\Sigma)$. The solution Γ is equivalent to a

path $(\gamma(x), e^{it(x)}) \in \Sigma \times S^1$ where

$$t(x) = \int_\gamma \tau$$

is obtained by integrating $dt - \tau$ along γ, setting the result equal to 0, and choosing $t(0) = 0$.

This solution defines a local Legendrian lift, $\tilde{f}$ of U into P. We get a global lift if

$$\int_\gamma \tau \in 2\pi\mathbb{Z} \quad \text{for all } [\gamma] \in H_1(\Sigma).$$

In this case, $f : \Sigma \to X$ lifts to a Legendrian immersion $\tilde{f} : \Sigma \to P$ (i.e., the local lift extends to all of Σ).

If integrating τ along any path joining a pair of double points results in a nonzero answer (mod 2π), then the lift $\tilde{f}$ is an embedding. We summarize the discussion above as follows:

Theorem 2.1. *Let Σ^n be a connected n-manifold, X^{2n} be a $2n$-dimensional symplectic manifold with integral symplectic form ω, and $f : \Sigma \to X$ be a Lagrangian immersion. Let $\pi : P \to X$ be the principle S^1-bundle with connection 1-form $i\eta$ determined by $d\eta = \pi^*(\omega)$. Suppose the section $\sigma : \Sigma \to f^*(P)$ defines coordinates (x, e^{it}) of the trivial bundle $F : f^*(P) \to P$ such that $F^*(\eta) = k(dt - \tau)$ where $k \in \mathbb{R}$ is a constant and $\tau \in \Omega^1(\Sigma)$. If*

(1) $\int_\gamma \tau \in 2\pi\mathbb{Z}$ *for all* $[\gamma] \in H_1(\Sigma; \mathbb{Z})$, *and*

(2) *for all points $x_0, x_1 \in \Sigma$ such that $f(x_0) = f(x_1)$ and any path γ from x_0 to x_1 in Σ, $\int_\gamma \tau \neq 0 \bmod 2\pi$,*

then $f : \Sigma \to X$ lifts to $\tilde{f} : \Sigma \to P$ and the image (the lift) $\tilde{\Sigma}$ is a Legendrian submanifold of P.

Theorem 2.1 is general in that it describes exactly when immersions can be lifted, but it is far from helpful in describing how to construct such lifts by hand (or with the help of a computer). For example, given a symplectic manifold X, like $\mathbb{C}P^n$ (or T^n, $E(n)$, $\mathrm{Sym}^n(\Sigma_g)$, etc), what chart system should we use to make the calculation easiest? (Note the standard chart system $U_i = \{[z_1 : \cdots : 1 : \cdots : z_n] | z_i \in \mathbb{C}\} \subset \mathbb{C}P^{n-1}$ is not convenient for constructing lifts.)

Can a chart system of X be chosen in such a way that the symplectic form ω is standard in each chart? Can a chart system be chosen so that the principal S^1-bundle trivializes over each chart in such a way that η has a nice (simple) form in each trivialization, and there is an obvious choice of sections so that τ also has a nice representation? None of these questions are answered by Theorem 2.1 (because they are specific to X), but all of them are important to being able to generate

explicit examples of lifts that satisfy the restrictive requirements needed to be able to compute invariants like the Legendrian contact homology of the lifts.

For these reasons, the following theorem is useful to us in computing the invariants of Lagrangian cones in $\mathbb{C}^n$ in this paper.

Theorem 2.2. *Let $B^{n-1} \subset \mathbb{C}^{n-1}$ be a ball, Σ be a closed, connected, smooth $(n-1)$-manifold, and $f : \Sigma \to B^{n-1}$ be a Lagrangian immersion with respect to the standard symplectic form ω_0 of $\mathbb{C}^{n-1}$. Let $\tau = -\sum_{i=1}^{n-1}(x_i dy_i - y_i dx_i)$ be a 1-form on B^{n-1}. If*

(1) *$\int_{f(\gamma)} \tau \in 2\pi\mathbb{Z}$ for all $\gamma \in H_1(\Sigma; \mathbb{Z})$, and*
(2) *for all distinct points $x_1, \dots, x_k \in \Sigma$ such that $f(x_1) = f(x_j)$ for all $j \le k$, and a choice of path γ_j from x_1 to x_j in Σ for $2 \le j \le k$, the set $\left\{\left(\int_{f(\gamma_j)} \tau\right) \bmod 2\pi \mid 2 \le j \le k\right\}$ has $k-1$ distinct values, none of which are equal to 0,*

then Σ lifts to an embedded Legendrian submanifold $\tilde{\Sigma} \subset S^{2n-1}$ whose associated cone $c\tilde{\Sigma}$ is Lagrangian in $\mathbb{C}^n$.

The lift, $\tilde{f} : \Sigma \to S^{2n-1} \subset \mathbb{C}^n$, is given by

$$\tilde{f}(x) = e^{it(x)}(f_1(x), \dots, f_{n-1}(x), \sqrt{1 - |f(x)|^2})$$

where

$$t(x) = \int_{f(\gamma)} \tau$$

for some path γ from an initial point $x_0 \in \Sigma$ to x.

Careful comparison of the calculations in Theorem 2.2 with those of Theorem 2.1 shows that Theorem 2.2 is the realization of Theorem 2.1 in the case where Σ^{n-1} is an immersion into an open unit ball, thought of as a single chart of $\mathbb{C}P^{n-1}$ (and where we do the calculations in the chart, instead of in Σ). For a proof of Theorem 2.2, see Section 4, where we prove the lifting theorem, which is a more general version of this theorem.

3. Examples of lifts using Theorem 2.2

3A. *Legendrian contact homology generators for the Harvey–Lawson cone.*

Example 3.1. Theorem 2.2 allows us to construct a family of isotopies of the famous special Lagrangian cone given by Harvey and Lawson (see Example 1.5). Choose ϵ so that $0 \le \epsilon < \sqrt{2/n}$ and define $\delta = \sqrt{1/n - \epsilon^2/2}$. Parametrize the torus T^{n-1} in the usual way with coordinates $(\theta_1, \dots, \theta_{n-1}) \in \mathbb{R}^{n-1}$. Let $r_\epsilon(\theta_1, \dots, \theta_{n-1}) = \delta + \epsilon \sin(\theta_1 + \cdots + \theta_{n-1})$, and define $f_\epsilon : T^{n-1} \to B^{n-1}$ by

$$f_\epsilon(\theta_1, \dots, \theta_{n-1}) = \left(r_\epsilon(\theta_1, \dots, \theta_{n-1}) e^{i(2\theta_1 + \theta_2 + \cdots + \theta_{n-1})}, \dots, r_\epsilon(\theta_1, \dots, \theta_{n-1}) e^{i(\theta_1 + \cdots + \theta_{n-2} + 2\theta_{n-1})}\right).$$

Observe that the first condition of Theorem 2.2 is satisfied. Thus, defining $t(x)$ as in Theorem 2.2, we obtain a family of Legendrian tori in $S^{2n-1} \subset \mathbb{C}^n$, each of whose associated cones are Lagrangian, given by the maps

$$\tilde{f}_\epsilon(\theta_1, \dots, \theta_{n-1}) = e^{it_\epsilon(\theta_1,\dots,\theta_{n-1})} \times \Big(r_\epsilon(\theta_1, \dots, \theta_{n-1}) e^{i(2\theta_1+\theta_2+\cdots+\theta_{n-1})}, \dots, r_\epsilon(\theta_1, \dots, \theta_{n-1}) e^{i(\theta_1+\cdots+\theta_{n-2}+2\theta_{n-1})}, \sqrt{1-(n-1)r_\epsilon^2} \Big),$$

where

$$t_\epsilon(\theta_1, \dots, \theta_{n-1}) = \int_{f_\epsilon(\gamma)} \tau,$$

as in Theorem 2.2.

Remark 3.2. The cone on the image of the lift $\tilde{f}_\epsilon$ is Lagrangian for all $\epsilon \geq 0$, but is also special Lagrangian when $\epsilon = 0$. In fact, when $\epsilon = 0$, the associated cone is the Harvey–Lawson cone (see Example 1.5).

Theorem 3.3. *The parameter t_ϵ is given by*

$$t_\epsilon(\theta_1, \dots, \theta_{n-1}) = -(\theta_1+\cdots+\theta_{n-1}) - 2n\delta\epsilon(1-\cos(\theta_1+\cdots+\theta_{n-1})) + \frac{n}{4}\epsilon^2 \sin(2(\theta_1+\cdots+\theta_{n-1})).$$

Proof. For simplicity, we work in polar coordinates and integrate the pull-back $f_\epsilon{}^*(\tau) = -n \sum_{i=1}^{n-1} r_i^2 d\theta_i$ over a path in the torus T^{n-1} for the computation below. Taking γ_i to be a path from $(\theta_1, \dots, \theta_{i-1}, 0, \dots, 0)$ to $(\theta_1, \dots, \theta_{i-1}, \theta_i, 0, \dots, 0)$, and γ to be the concatenation of these paths from $i = 1, \dots, n$, then we may solve for t_ϵ as follows:

$$\begin{aligned} t_\epsilon(\theta_1, \dots, \theta_{n-1}) &= -n \sum_{i=1}^{n-1} \int_0^{\theta_i} r_\epsilon(\theta_1, \dots, \theta_{i-1}, \alpha_i, 0, \dots, 0)^2 d\alpha_i \\ &= -n \sum_{i=1}^{n-1} \Big[\Big(\tfrac{1}{2}(2\delta^2+\epsilon^2)\alpha_i - 2\delta\epsilon \cos(\theta_1+\cdots+\theta_{i-1}+\alpha_i) \\ &\qquad - \tfrac{1}{4}\epsilon^2 \sin(2(\theta_1+\cdots+\theta_{i-1}+\alpha_i)) \Big) \Big|_0^{\theta_i} \Big] \end{aligned}$$

Observe that the sum above telescopes, and hence, we may write

$$\begin{aligned} t_\epsilon(\theta_1, \dots, \theta_{n-1}) &= -n\Big(\tfrac{1}{2}(2\delta^2+\epsilon^2)(\theta_1+\cdots+\theta_{n-1}) - 2\delta\epsilon(1-\cos(\theta_1+\cdots+\theta_{n-1})) \\ &\qquad - \tfrac{1}{4}\epsilon^2 \sin(2(\theta_1+\cdots+\theta_{n-1})) \Big) \\ &= -(\theta_1+\cdots+\theta_{n-1}) - 2n\delta\epsilon(1-\cos(\theta_1+\cdots+\theta_{n-1})) \\ &\qquad + \frac{n}{4}\epsilon^2 \sin(2(\theta_1+\cdots+\theta_{n-1})). \qquad \square \end{aligned}$$

In light of Theorem 3.3, we get the following corollary.

Corollary 3.4. *As* $\epsilon \to 0$, $\delta \to 1/\sqrt{n}$, $t_\epsilon(\theta_1, \ldots, \theta_{n-1}) \to t_0(\theta_1, \ldots, \theta_{n-1}) = -\theta_1 - \cdots - \theta_{n-1}$, *and*

$$\tilde{f}_\epsilon(\theta_1, \ldots, \theta_{n-1}) \to \tilde{f}_0(\theta_1, \ldots, \theta_{n-1}) = \frac{1}{\sqrt{n}}(e^{i\theta_1}, \ldots, e^{i\theta_{n-1}}, e^{-i(\theta_1+\cdots+\theta_{n-1})}).$$

In order to verify that the second condition of Theorem 2.2 is satisfied, and consequently that the lift is embedded, we will be interested in locating the double points of f_ϵ.

Because we are mainly interested in cones of $\mathbb{C}^3$ via the SYZ conjecture, we assume $n = 3$ in the following calculation. Lemma 3.5 specifies precisely when the arguments of the exponential maps in the definition of f_ϵ all agree, a necessary condition for a double point.

Lemma 3.5. *For* $n = 3$, *if* $f_\epsilon(\theta_1, \theta_2) = f_\epsilon(\gamma_1, \gamma_2)$ *then* $\theta_1 = \gamma_1$ *and* $\theta_2 = \gamma_2$, *or* $\theta_1 - \gamma_1 = \theta_2 - \gamma_2 = \frac{2\pi}{3} \pmod{2\pi}$ *or* $\theta_1 - \gamma_1 = \theta_2 - \gamma_2 = \frac{4\pi}{3} \pmod{2\pi}$.

Proof. If $f_\epsilon(\theta_1, \theta_2) = f_\epsilon(\gamma_1, \gamma_2)$ then since the arguments of the exponential maps differ by a multiple of 2π, (θ_1, θ_2) and (γ_1, γ_2) must satisfy the equations

$$2\theta_1 + \theta_2 = 2\gamma_1 + \gamma_2 + n2\pi, \tag{3-1}$$

$$\theta_1 + 2\theta_2 = \gamma_1 + 2\gamma_2 + m2\pi, \tag{3-2}$$

for some $m, n \in \mathbb{Z}$.

Solving (3-1) and (3-2), we obtain the following:

$$\theta_1 - \gamma_1 = \frac{2n - m}{3}2\pi, \tag{3-3}$$

$$\theta_2 - \gamma_2 = \frac{2m - n}{2}\pi. \tag{3-4}$$

Since the torus T^2 is parametrized by $(\theta_1, \theta_2) \in [0, 2\pi) \times [0, 2\pi)$, it must be that $\theta_i - \gamma_i < 2\pi$ for $i = 1, 2$, and hence $\left|\frac{2m-n}{3}\right| < 1$ and $\left|\frac{2n-m}{3}\right| < 1$.

Since $n, m \in \mathbb{Z}$, we find that the possibilities for (n, m) are $\pm(1, 0)$, $\pm(0, 1)$, $\pm(1, 1)$ and $(0, 0)$. Evaluating (3-3) and (3-4), we find that either $\theta_1 = \gamma_1$ and $\theta_2 = \gamma_2$, or $\theta_1 - \gamma_1 = \theta_2 - \gamma_2 = \frac{2\pi}{3} \pmod{2\pi}$ or $\theta_1 - \gamma_1 = \theta_2 - \gamma_2 = \frac{4\pi}{3} \pmod{2\pi}$. □

In the proof above we also showed, after taking limits, that:

Scholium 3.6. *The image of* $\tilde{f}_0$ *is a* 3*-fold cover of the image of* f_0 *via the projection given by the Hopf map.*

Lemma 3.5 specifies when the arguments of the exponential maps will agree, but for a double point, the radii, determined by r_ϵ must also agree. In the following lemma, we calculate where this occurs.

Lemma 3.7. *If* $f_\epsilon(\theta_1, \theta_2) = f_\epsilon(\gamma_1, \gamma_2)$ *and either* $\theta_1 - \gamma_1 = \theta_2 - \gamma_2 = \frac{2\pi}{3} \pmod{2\pi}$ *or* $\theta_1 - \gamma_1 = \theta_2 - \gamma_2 = \frac{4\pi}{3} \pmod{2\pi}$, *then one of the following must be true*:

- $\theta_1 + \theta_2 = \gamma_1 + \gamma_2$.
- $\theta_1 + \theta_2 = \frac{7\pi}{6}$ *and* $\gamma_1 + \gamma_2 = \frac{11\pi}{6}$.
- $\theta_1 + \theta_2 = \frac{5\pi}{6}$ *and* $\gamma_1 + \gamma_2 = \frac{\pi}{6}$.

Proof. Since $f_\epsilon(\theta_1, \theta_2) = f_\epsilon(\gamma_1, \gamma_2)$, not only must the arguments of the exponential maps differ by a multiple of 2π, but the radii in each complex factor must match, that is $r_\epsilon(\theta_1, \theta_2) = r_\epsilon(\gamma_1, \gamma_2)$. Hence one of the following equations must hold:

$$\theta_1 + \theta_2 = \gamma_1 + \gamma_2, \tag{3-5}$$

$$\theta_1 + \theta_2 + \gamma_1 + \gamma_2 = \pi + 2\pi k. \tag{3-6}$$

There are several cases. If $\theta_1 + \theta_2 = \gamma_1 + \gamma_2$, then using (3-3) and (3-4), one can show that $n = -m$ which can only happen if $n = m = 0$. Furthermore, if $\theta_1 + \theta_2 + \gamma_1 + \gamma_2 = \pi + k2\pi$, combining this with (3-3) and (3-4), we may solve the system to obtain that $\theta_1 + \theta_2 = \frac{7\pi}{6}$ and $\gamma_1 + \gamma_2 = \frac{11\pi}{6}$ or $\theta_1 + \theta_2 = \frac{5\pi}{6}$ and $\gamma_1 + \gamma_2 = \frac{\pi}{6}$. □

Remark 3.8. Lemma 3.5 rules out the possibility of multiple points of f_ϵ of multiplicity greater than 3, and Lemma 3.7 shows that for $\epsilon > 0$ there are no triple points. Hence, immersion f_ϵ has only double points when $\epsilon > 0$.

The families of double points identified in Lemma 3.7 form copies of S^1, and will show up not only in this example, but in others as well. Hence the following definition will be useful in some of the discussion that follows.

Definition 3.9. Let $f : \Sigma \to M$ be an immersion of a surface. Suppose C_1 and C_2 are disjoint copies of S^1 in Σ such that $f(C_1) = f(C_2)$ and $f|_{C_1 \cup C_2}$ is a 2-to-1 map. Suppose further that A_1 and A_2 are disjoint annular neighborhoods of C_1 and C_2 and that $f(A_1) \cap f(A_2) = f(C_1) = f(C_2)$. If, for any pair consisting of $x_1 \in C_1$ and $x_2 \in C_2$ such that $f(x_1) = f(x_2)$, we have that $df_{x_1}(TA_1) \neq df_{x_2}(TA_2)$, then we call the image of C_1 and C_2 a *double point circle*.

Theorem 3.10. *The double points of f_ϵ, of the form $f_\epsilon(\theta_1, \theta_2) = f_\epsilon(\gamma_1, \gamma_2)$, consist of two double point circles such that $\theta_1 - \gamma_1 = \theta_2 - \gamma_2 = \frac{2\pi}{3} \pmod{2\pi}$ or $\theta_1 - \gamma_1 = \theta_2 - \gamma_2 = \frac{4\pi}{3} \pmod{2\pi}$ and one of the following holds*:

(1) $\theta_1 + \theta_2 = \frac{7\pi}{6}$ *and* $\gamma_1 + \gamma_2 = \frac{11\pi}{6}$.

(2) $\theta_1 + \theta_2 = \frac{5\pi}{6}$ *and* $\gamma_1 + \gamma_2 = \frac{\pi}{6}$.

Proof. Lemmas 3.5 and 3.7 demonstrate that systems of this type yield double points. All that remains is the observation that if (θ_1, θ_2) and (γ_1, γ_2) satisfy $\theta_1 - \gamma_1 = \theta_2 - \gamma_2 = \frac{2\pi}{3} \pmod{2\pi}$ or $\theta_1 - \gamma_1 = \theta_2 - \gamma_2 = \frac{4\pi}{3} \pmod{2\pi}$ but do not satisfy either (1) or (2), then $\sin(\theta_1 + \theta_2) \neq \sin(\gamma_1 + \gamma_2)$. For such cases, $r_\epsilon(\theta_1, \theta_2) \neq r_\epsilon(\gamma_1, \gamma_2)$ and hence $f_\epsilon(\theta_1, \theta_2) \neq f_\epsilon(\gamma_1, \gamma_2)$. □

Theorem 3.11. *The lift $\tilde{f}_\epsilon$ is an embedding.*

Proof. We already know the lift is well defined. All that remains is to check that the second condition of Theorem 2.2 is satisfied, which means that the double points of the projection are separated in the lift. This amounts to computing $\int_{f(\gamma)} \tau$ for some path γ joining a pair of double points of a double point circle. Using Theorem 3.10, suppose we have a double point such that $f_\epsilon(\theta_1, \frac{5\pi}{6} - \theta_1) = f_\epsilon\big(\theta_1 + \frac{2\pi}{3}, \frac{13\pi}{6} - \big(\theta_1 + \frac{2\pi}{3}\big)\big)$. Then the integral in question is given by:

$$t_\epsilon\left(\theta_1 + \frac{2\pi}{3}, \frac{13\pi}{6} - \left(\theta_1 + \frac{2\pi}{3}\right)\right) - t_\epsilon\left(\theta_1, \frac{5\pi}{6} - \theta_1\right).$$

Using the expression for t_ϵ given in Theorem 3.3, and simplifying, we obtain

$$t_\epsilon\left(\theta_1 + \frac{2\pi}{3}, \frac{13\pi}{6} - \left(\theta_1 + \frac{2\pi}{3}\right)\right) - t_\epsilon\left(\theta_1, \frac{5\pi}{6} - \theta_1\right)$$
$$= -\frac{8\pi}{6} - 4n\delta\epsilon\cos\left(\frac{5\pi}{6}\right) + \frac{n\epsilon^2}{2}\sin\left(\frac{\pi}{3}\right).$$

Noting that $n = 3$, $0 \le \epsilon < \sqrt{2/3}$, and $\delta = \sqrt{1/3 - \epsilon^2/2}$, we have that

$$-\frac{4\pi}{3} \le t_\epsilon\left(\theta_1 + \frac{2\pi}{3}, \frac{13\pi}{6} - \left(\theta_1 + \frac{2\pi}{3}\right)\right) - t_\epsilon\left(\theta_1, \frac{5\pi}{6} - \theta_1\right) < -\frac{4\pi}{3} + \frac{\sqrt{3}}{2}.$$

The other double points are handled in a similar manner. □

Let L_ϵ be the image of f_ϵ and let $\tilde{L}_\epsilon$ be the Legendrian torus given by the lift $\tilde{f}_\epsilon$. We wish to identify the generators of the 0-filtration level of the Legendrian contact homology of $\tilde{L}_\epsilon$, which are determined by the double points of the Lagrangian projection. Recall that in this case, the double points are actually double point circles, hence we need to perturb the map so that it is chord-generic. We will demonstrate the perturbation for $n = 3$, but the general solution is similar.

Lemma 3.12. *Let $\tilde{f}_\epsilon : T^2 \to S^5$ be the Legendrian torus given by the map*

$$\tilde{f}_\epsilon(\theta_1, \theta_2) = e^{it_\epsilon(\theta_1,\theta_2)}\Big(r_\epsilon(\theta_1, \theta_2)e^{i(2\theta_1+\theta_2)}, r_\epsilon(\theta_1, \theta_2)e^{i(\theta_1+2\theta_2)}, \sqrt{1 - 2r_\epsilon(\theta_1, \theta_2)^2}\Big).$$

Choose a perturbation in the direction of the Reeb fiber, $s_\epsilon : T^2 \to S^1$, two perturbations in the radial directions, $s_{i,\epsilon} : T^2 \to \mathbb{R}$, for $i = 1, 2$, and define

$$\tilde{g}_\epsilon(\theta_1, \theta_2)$$
$$= e^{i(t_\epsilon(\theta_1,\theta_2)+s_\epsilon(\theta_1,\theta_2))}\Big(r_{1,\epsilon}(\theta_1, \theta_2)e^{i(2\theta_1+\theta_2)}, r_{2,\epsilon}(\theta_1, \theta_2)e^{i(\theta_1+2\theta_2)}, \sqrt{1-r_{1,\epsilon}^2-r_{2,\epsilon}^2}\Big),$$

where $r_{i,\epsilon}(\theta_1, \theta_2) = r_\epsilon(\theta_1, \theta_2) + s_{i,\epsilon}(\theta_1, \theta_2)$ for $i = 1, 2$. If

(1) $\frac{\partial s_\epsilon}{\partial \theta_1} + 2r_\epsilon(\theta_1, \theta_2)(2s_{1,\epsilon}(\theta_1, \theta_2) + s_{2,\epsilon}(\theta_1, \theta_2)) + 2s_{1,\epsilon}(\theta_1, \theta_2)^2 + s_{2,\epsilon}(\theta_1, \theta_2)^2 = 0$ *and*

(2) $\frac{\partial s_\epsilon}{\partial \theta_2} + 2r_\epsilon(\theta_1, \theta_2)(s_{1,\epsilon}1(\theta_1, \theta_2) + 2s_{2,\epsilon}(\theta_1, \theta_2)) + s_{1,\epsilon}(\theta_1, \theta_2)^2 + 2s_{2,\epsilon}(\theta_1, \theta_2)^2 = 0$

then the perturbation $\tilde{g}_\epsilon$ is a Legendrian torus having only transverse double points that is Legendrian isotopic to $\tilde{f}_\epsilon$.

Moreover, for a given choice of s_ϵ the system is solved by

$$s_{1,\epsilon}(\theta_1,\theta_2) = -r_\epsilon(\theta_1,\theta_2) + \sigma\sqrt{r_\epsilon(\theta_1,\theta_2)^2 + \frac{1}{3}\left(\frac{\partial s_\epsilon}{\partial\theta_2} - 2\frac{\partial s_\epsilon}{\partial\theta_1}\right)}$$

and

$$s_{2,\epsilon}(\theta_1,\theta_2) = -r_\epsilon(\theta_1,\theta_2) + \sigma\sqrt{r_\epsilon(\theta_1,\theta_2)^2 + \frac{1}{3}\left(\frac{\partial s_\epsilon}{\partial\theta_1} - 2\frac{\partial s_\epsilon}{\partial\theta_2}\right)},$$

where σ is ± 1.

Proof. The calculation is easiest if we work in polar coordinates and identify a neighborhood of the $\tilde{f}_\epsilon$ with $B_2 \times S^1$ (cf. the lifting theorem). Note that we may write

$$\tilde{f}_\epsilon(\theta_1,\theta_2) = \big(r_\epsilon(\theta_1,\theta_2), 2\theta_1+\theta_2, r_\epsilon(\theta_1,\theta_2), \theta_1+2\theta_2, t_\epsilon(\theta_1,\theta_2)\big),$$

and we work with the perturbation in polar coordinates as well:

$$\tilde{g}_\epsilon(\theta_1,\theta_2) = \big(r_{1,\epsilon}(\theta_1,\theta_2), 2\theta_1+\theta_2, r_{2,\epsilon}(\theta_1,\theta_2), \theta_1+2\theta_2, t_\epsilon(\theta_1,\theta_2)+s_\epsilon(\theta_1,\theta_2)\big),$$

In these coordinates, we may identify the contact form α on S^5 with $\frac{1}{2}(dt-\tau)$ (for details of this calculation see the lifting theorem). Pulling back α to T^2 via $\tilde{f}_\epsilon$ we obtain the form

$$\tilde{f}_\epsilon^*(\alpha) = \left(\frac{\partial t_\epsilon}{\partial\theta_1} + 3r_\epsilon(\theta_1,\theta_2)^2\right)d\theta_1 + \left(\frac{\partial t_\epsilon}{\partial\theta_2} + 3r_\epsilon(\theta_1,\theta_2)^2\right)d\theta_2.$$

Since $\tilde{f}_\epsilon$ is Legendrian, this is 0, and hence

$$\left(\frac{\partial t_\epsilon}{\partial\theta_1} + 3r_\epsilon(\theta_1,\theta_2)^2\right) = \left(\frac{\partial t_\epsilon}{\partial\theta_2} + 3r_\epsilon(\theta_1,\theta_2)^2\right) = 0.$$

Pulling back α using the perturbation $\tilde{g}_\epsilon$ we obtain

$$\begin{aligned}\tilde{g}_\epsilon^*(\alpha) = &\left[\left(\frac{\partial t_\epsilon}{\partial\theta_1}+3r_\epsilon(\theta_1,\theta_2)^2\right)+\frac{\partial s_\epsilon}{\partial\theta_1}+2r_\epsilon(\theta_1,\theta_2)(2s_{1,\epsilon}+s_{2,\epsilon})+2s_{1,\epsilon}^2+s_{2,\epsilon}^2\right]d\theta_1\\ &+\left[\left(\frac{\partial t_\epsilon}{\partial\theta_2}+3r_\epsilon(\theta_1,\theta_2)^2\right)\frac{\partial s_\epsilon}{\partial\theta_2}+2r_\epsilon(\theta_1,\theta_2)(s_{1,\epsilon}+2s_{2,\epsilon})+s_{1,\epsilon}^2+2s_{2,\epsilon}^2\right]d\theta_2.\end{aligned}$$

Noting that $\left(\frac{\partial t_\epsilon}{\partial\theta_1}+3r_\epsilon(\theta_1,\theta_2)^2\right) = \left(\frac{\partial t_\epsilon}{\partial\theta_2}+3r_\epsilon(\theta_1,\theta_2)^2\right) = 0$, we have justified (1) and (2). The last part is routine, and obtained by solving this system of equations, (1) and (2), for $s_{1,\epsilon}$ and $s_{2,\epsilon}$. □

Theorem 3.13. *The map $g_\epsilon : T^2 \to B^2$,*

$$g_\epsilon(\theta_1,\theta_2) = (r_{1,\epsilon}(\theta_1,\theta_2)e^{i(2\theta_1+\theta_2)}, r_{2,\epsilon}(\theta_1,\theta_2)e^{i(\theta_1+2\theta_2)}),$$

where

$$r_{1,\epsilon}(\theta_1,\theta_2)=\sqrt{r_\epsilon(\theta_1,\theta_2)^2-\tfrac{2}{3}\epsilon\cos(\theta_1)}\quad\text{and}\quad r_{2,\epsilon}(\theta_1,\theta_2)=\sqrt{r_\epsilon(\theta_1,\theta_2)^2+\tfrac{1}{3}\epsilon\cos(\theta_1)}$$

is a perturbation of f_ϵ having exactly two transverse double points. Moreover, the lift $\tilde{g}_\epsilon$,

$$\begin{aligned}&\tilde{g}_\epsilon(\theta_1,\theta_2)\\&=e^{i(t_\epsilon(\theta_1,\theta_2)+s_\epsilon(\theta_1,\theta_2))}\Big(r_{1,\epsilon}(\theta_1,\theta_2)e^{i(2\theta_1+\theta_2)},\, r_{2,\epsilon}(\theta_1,\theta_2)e^{i(\theta_1+2\theta_2)},\,\sqrt{1-r_{1,\epsilon}^2-r_{2,\epsilon}^2}\Big),\end{aligned}$$

is Legendrian isotopic to $\tilde{f}_\epsilon$.

Proof. Choose $s_\epsilon(\theta_1,\theta_2)=\epsilon\sin(\theta_1)$. Direct calculation shows that the conditions of Lemma 3.12 are satisfied. Moreover, the two maps $s_{1,\epsilon}$ and $s_{2,\epsilon}$ from Lemma 3.12 satisfy the following:

(1) $r_{1,\epsilon}(\theta_1,\theta_2)=r_\epsilon(\theta_1,\theta_2)+s_{1,\epsilon}(\theta_1,\theta_2)=\sqrt{r_\epsilon(\theta_1,\theta_2)^2-\tfrac{2}{3}\epsilon\cos(\theta_1)}$.

(2) $r_{2,\epsilon}(\theta_1,\theta_2)=r_\epsilon(\theta_1,\theta_2)+s_{2,\epsilon}(\theta_1,\theta_2)=\sqrt{r_\epsilon(\theta_1,\theta_2)^2+\tfrac{1}{3}\epsilon\cos(\theta_1)}$.

The remainder follows from Lemma 3.12. □

The following corollary is obvious:

Corollary 3.14. *Taking the limit as $\epsilon\to 0$, we have the following*:

(1) $t_\epsilon(\theta_1,\theta_2)\to t_0(\theta_1,\theta_2)=-\theta_1-\theta_2$.

(2) $\tilde{g}_\epsilon(\theta_1,\theta_2)\to\tilde{g}_0(\theta_1,\theta_2)=\tilde{f}_0(\theta_1,\theta_2)=\frac{1}{\sqrt{2}}(e^{i\theta_1},e^{i\theta_2},e^{-i(\theta_1+\theta_2)})$.

Corollary 3.14 shows that $\tilde{g}_0$ is the Harvey–Lawson cone (just as $\tilde{f}_0$ is). What makes $\tilde{g}_\epsilon$ useful is that although it is isotopic to the Harvey–Lawson cone, it has isolated double points. In fact, it has only four transverse double points as observed in the following corollary.

Corollary 3.15. *The double points of g_ϵ can be found directly, and we obtain* 2 *for each double point circle, for a total of four transverse double points*:

(1) $g_\epsilon\big(\frac{2\pi}{3},\frac{\pi}{6}\big)=g_\epsilon\big(\frac{4\pi}{3},\frac{5\pi}{6}\big)$,

(2) $g_\epsilon\big(\frac{5\pi}{3},\frac{7\pi}{6}\big)=g_\epsilon\big(\frac{\pi}{3},\frac{11\pi}{6}\big)$,

(3) $g_\epsilon\big(\frac{2\pi}{3},\frac{7\pi}{6}\big)=g_\epsilon\big(\frac{4\pi}{3},\frac{11\pi}{6}\big)$, *and*

(4) $g_\epsilon\big(\frac{5\pi}{3},\frac{\pi}{6}\big)=g_\epsilon\big(\frac{\pi}{3},\frac{5\pi}{6}\big)$.

Proof. Writing g_ϵ in polar coordinates, as in Lemma 3.5, we see that any double points must be of the form $g_\epsilon(\theta_1,\theta_2)=g_\epsilon(\theta_1+j\frac{2\pi}{3},\theta_2+j\frac{2\pi}{3})$ where j is either 1 or 2, in order that the arguments of the exponential maps both differ by a multiple

of 2π. Thus we get double points when we have the following two equations satisfied:

$$r_{1,\epsilon}(\theta_1, \theta_2) = r_{1,\epsilon}\left(\theta_1 + j\frac{2\pi}{3}, \theta_2 + j\frac{2\pi}{3}\right).$$
$$r_{2,\epsilon}(\theta_1, \theta_2) = r_{2,\epsilon}\left(\theta_1 + j\frac{2\pi}{3}, \theta_2 + j\frac{2\pi}{3}\right).$$

Solving this system of equations, we obtain the result. □

In summary, we have constructed a family of cones, each of which is isotopic to the Harvey–Lawson cone, but with the additional property that the projection to $\mathbb{C}P^2$ has only four transverse double points, unlike the actual Harvey–Lawson cone which is a 3-fold cover of its projection to $\mathbb{C}P^2$, as observed in Scholium 3.6. Although the isotopy taking the Harvey–Lawson cone to one of our perturbations does not preserve the special Lagrangian conditions, it does preserve the Legendrian link, and hence, can be used to calculate a suitably defined Legendrian contact homology [30]. Moreover, our perturbations have only transverse double points. Thus we obtain:

Theorem 3.16. *Let $T^2 \subset S^5$ be the torus constructed above, which is Legendrian isotopic to $T^+ \subset S^5$. Then the 0-filtration level of the Legendrian contact homology of T^2 is generated by four pairs of short Reeb chords, two each in gradings 4, 6, 7, and 9. These Reeb chords correspond to the double points of T^2 via the projection of T^2 under $\pi : S^5 \to \mathbb{C}P^2$.*

Remark 3.17. The lifting theorem made it possible to compute the gradings of Theorem 3.16 explicitly in Mathematica. By working in a single chart, we integrate to define the lift, and compute a unitary Lagrangian frame to obtain the Maslov index. The calculations, though long, are straightforward and therefore omitted.

Remark 3.18. While the Legendrian contact homology of the Harvey–Lawson cone is beginning to emerge in the previous theorem, it does not take into account the Reeb chords that wrap around the fiber. However, considering the gradings of the short chords, it does appear that there is nontrivial homology in gradings 4 and 9.

3B. ***Lagrangian hypercube diagrams.*** Next, we show how to generalize the calculations above to get knotted Legendrian tori in S^5 (knotted in the sense that they are the product of two Legendrian knots in $\mathbb{R}^3$; see [4]). The cones on these knotted tori are Lagrangian cones in $\mathbb{C}^3$. Therefore we begin the study of diagrammatic Lagrangian cones in $\mathbb{C}^3$.

In [4], Lagrangian hypercube diagrams were used to produce examples of Legendrian tori in the standard contact space, $(\mathbb{R}^5, \xi_{std})$, using $wxyzt$-coordinates on $\mathbb{R}^5$

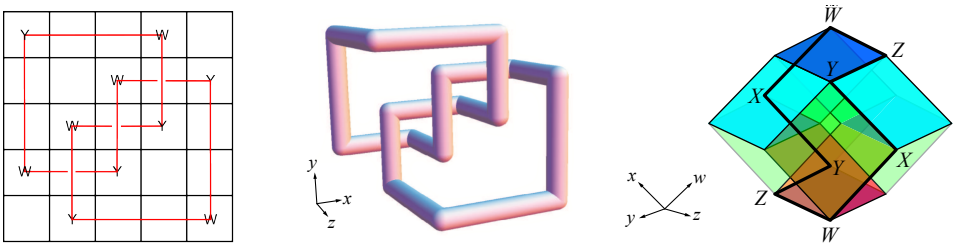

Figure 1. Grid and cube diagrams for the trefoil, and a hypercube diagram for a torus.

and letting $\xi_{std} = dt - ydw - xdz$. But they can also be adapted to produce Legendrian tori in S^5 whose cones in $\mathbb{C}^3$ are Lagrangian. Before doing so, we briefly recall some of the relevant material from [4] and refer the reader to that paper for more details.

Lagrangian hypercube diagrams are closely related to grid, cube, and hypercube diagrams. To construct a grid, cube, or hypercube diagram, one places markings in a 2-, 3-, or 4-dimensional Cartesian grid, while ensuring that certain marking conditions and crossing conditions hold (see Section 2 and 3 in [2], and Section 2 in [3]). In each case, the markings determine a link (see Figure 1). For a hypercube diagram, there is an algorithm for constructing a Lagrangian torus associated to the hypercube diagram, such as the one shown in the last picture in Figure 1 (see Theorem 5.1 in [2]).

In order to define a Lagrangian hypercube diagram, we first need to define a Lagrangian grid diagram:

Definition 3.19. A *Lagrangian grid diagram* given by $\gamma : S^1 \to \mathbb{R}^2$ where $\gamma(\theta) = (x(\theta), y(\theta))$ is an immersed grid diagram G satisfying conditions (3-7) and (3-8):

$$\int_0^{2\pi} y(\theta)x'(\theta)d\theta = 0, \tag{3-7}$$

$$\int_{\theta_0}^{\theta_1} y(\theta)x'(\theta)d\theta \neq 0 \text{ whenever } \gamma(\theta_0) = \gamma(\theta_1) \text{ and } 0 < \theta_1 - \theta_0 < 2\pi. \tag{3-8}$$

While any Lagrangian projection of a Legendrian knot satisfies (3-7) and (3-8), it is usually difficult to determine from a given diagram in the plane whether or not the diagram will lift to a Legendrian knot. The advantage with a Lagrangian grid diagram is that one merely needs to add up the signed areas of a finite number of rectangles to determine whether the diagram lifts to a Legendrian knot (see Corollary 3.10, Scholium 3.12 and Corollary 3.13 in [4]).

A Lagrangian hypercube diagram takes two Lagrangian grid diagrams and uses them to construct a *product* of two Legendrian knots (see [4] and [16]). To construct a grid diagram, one places markings in a 2-dimensional grid, subject to a set of marking conditions, and creates a knot diagram by drawing segments, joining

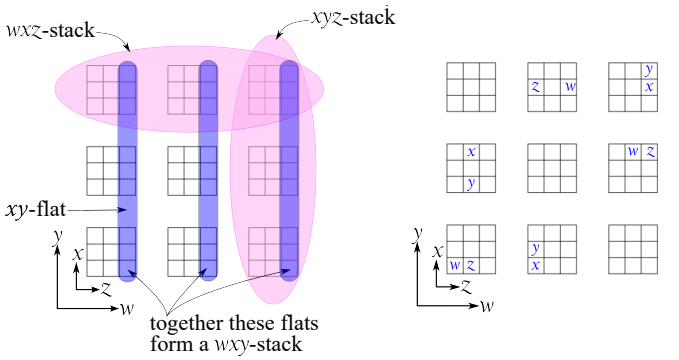

Figure 2. A schematic for displaying a Lagrangian hypercube diagram. The outer w and y coordinates indicate the "level" of each zx-flat. The inner z and x coordinates start at $(0, 0)$ for each of the nine zx-flats. With these conventions understood, one can display xy-flats, xyz-stacks, wxz-stacks, wxy-stacks, etc. The second picture is a schematic of a Lagrangian hypercube diagram.

the markings to create immersed loops. The process of creating a Lagrangian hypercube diagram is similar: there is a set of marking conditions that determine how to place markings in a 4-dimensional Cartesian grid, and the markings are joined by segments, following an algorithm to create a simple loop. Before stating the conditions, we give a few preliminaries.

A *flat* is any right rectangular 4-dimensional polytope with integer valued vertices in C such that there are two orthogonal edges at a vertex of length n and the remaining two orthogonal edges are of length 1. (Each flat is congruent to the product of a unit square and an $n \times n$ square.) Moreover, the flat will be named by the two edges of length n. Although a flat is a 4-dimensional object, the name references the fact that a flat is a 2-dimensional array of unit hypercubes. For example, an xy-flat is a flat that has a face that is an $n \times n$ square that is parallel to the xy-plane. In a hypercube of size $n = 3$, one example of a xy-flat would be the subset $[0, 1] \times [0, 3] \times [0, 3] \times [2, 3]$ (shown in Figure 2).

A *stack* is a set of n flats that form a right rectangular 4-dimensional polytope with integer vertices in C in which there are three orthogonal edges of length n at a vertex, and the remaining edge has length 1. (Each stack is the product of a cube with edges of length n and a unit interval.) A stack is named by the three edges of length n. An example of a wxz-stack in a hypercube of size 3 is the subset $[0, 3] \times [0, 3] \times [2, 3] \times [0, 3]$ (shown at the top of Figure 2). Further examples of flats and stacks may be found in Figure 2.

A marking is a labeled point in $\mathbb{R}^4$ with half-integer coordinates in C. Unit hypercubes of the 4-dimensional Cartesian grid will either be blank, or marked with a W, X, Y, or Z such that the following *marking conditions* hold:

(1) Each stack has exactly one W, one X, one Y, and one Z marking.

(2) Each stack has exactly two flats containing exactly three markings in each.

(3) For each flat containing exactly three markings, the markings in that flat form a right angle such that each ray is parallel to a coordinate axis.

(4) For each flat containing exactly three markings, the marking that is the vertex of the right angle is W if and only if the flat is a zw-flat, X if and only if the flat is a wx-flat, Y if and only if the flat is a xy-flat, and Z if and only if the flat is a yz-flat.

Condition (4) rules out the possibility of either wy-flats or a zx-flats with three markings (see Figure 2). As with oriented grid diagrams and cube diagrams, we obtain an oriented link from the markings by connecting each W marking to an X marking by a segment parallel to the w-axis, each X marking to a Y marking by a segment parallel to the x-axis, and so on.

Let $\pi_{xz}, \pi_{wy} : \mathbb{R}^4 \to \mathbb{R}^2$ be the natural projections, projecting out the x, z and w, y directions respectively. The projection $\pi_{xz}(C)$ produces an $n \times n$ square in the wy-plane. If we project the W and Y markings of the hypercube to this square as well, the markings satisfy the conditions for an immersed grid diagram, which we denote $G_{wy} := (\pi_{xz}(C), \pi_{xz}(\mathcal{W}), \pi_{xz}(\mathcal{Y}))$, where $\mathcal{W}$ and $\mathcal{Y}$ are the sets of W and Y markings, respectively. Similarly, we define $G_{zx} := (\pi_{wy}(C), \pi_{wy}(\mathcal{Z}), \pi_{wy}(\mathcal{X}))$, where $\mathcal{Z}$ and $\mathcal{X}$ are the sets of Z and X markings respectively.

In a grid diagram, one typically requires a crossing condition, namely that the vertical segment crosses over the horizontal segment. For a Lagrangian hypercube diagram, the crossing conditions are determined as follows. We require that the two immersed grid diagrams, G_{zx} and G_{wy}, are Lagrangian grid diagrams (that is, they satisfy conditions (3-7) and (3-8)). By Proposition 3.4 of [4], a Lagrangian grid diagram lifts to a smoothly embedded Legendrian knot. Hence the crossing conditions of the grid are determined by this lift. We require one additional *product lift condition* that the pair G_{zx} and G_{wy} must satisfy. In the definition below, $\Delta t(c)$ is the length of the Reeb chord associated to the crossing c).

Definition 3.20. For two Lagrangian grid diagrams, G_{wy} and G_{zx}, let $\mathcal{C} = \{c_i\}$ be the crossings in G_{zx} and $\mathcal{C}' = \{c_i'\}$ be the crossings in G_{wy}. The pair of grid diagrams is said to satisfy the *product lift condition* if $|\Delta t(c_i)| \neq |\Delta t(c_i')|$ for all i, j.

We are now ready to define a Lagrangian hypercube diagram (see [4]):

Definition 3.21. A *Lagrangian hypercube diagram*, which we denote by $H\Gamma = (C, \{\mathcal{W}, \mathcal{X}, \mathcal{Y}, \mathcal{Z}\}, G_{zx}, G_{wy})$, is a set of markings $\{\mathcal{W}, \mathcal{X}, \mathcal{Y}, \mathcal{Z}\}$ in C that satisfy

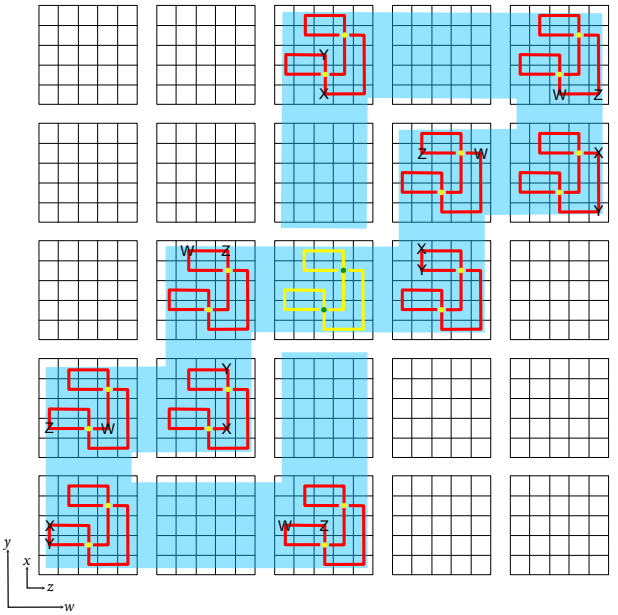

Figure 3. Lagrangian hypercube diagram with unknotted G_{zx} and G_{wy} and rotation class $(1, 0)$.

the marking conditions, where G_{wy} and G_{zx} are Lagrangian grid diagrams, and G_{wy} and G_{zx} satisfy the product lift condition.

The immersed torus specified by the Lagrangian hypercube diagram is the product of G_{zx} and G_{wy}, determined as follows: place a copy of the immersed grid G_{zx} at each zx-flat on the schematic that contains a pair of markings (shown in red on Figure 3). Doing so produces a schematic with two copies of G_{zx} with the same y-coordinates and two with the same w-coordinates. For each pair of copies sharing the same w-coordinates, we may translate one parallel to the w-axis toward the other. Doing so traces out an immersed tube connecting these two copies of G_{zx}. Similarly, we may translate parallel to the y-axis to produce an immersed tube connecting two copies of G_{zx} with the same y-coordinates. Since we are connecting copies of G_{zx} in flats corresponding to the markings of G_{wy}, the tube will close to produce an immersed torus.

3C. ***Lagrangian cones in $\mathbb{C}^3$ constructed from Lagrangian hypercube diagrams.*** First, we show how to convert a grid diagram to a *radial grid diagram*. A set of concentric circles $\{C_k\}_{k=1}^{n}$ of radius $\sqrt{k/(3n)}$ will serve to represent the rows of our grid, and a set of radial lines, determined by the list of angles, $\left\{k\frac{2\pi}{n}\right\}_{k=0}^{n-1}$, to serve as columns. The counterclockwise direction is chosen to correspond to the positive x-direction in the original grid, and the outward pointing radial direction is chosen to correspond to the positive y-direction. Moreover, the radii of the concentric

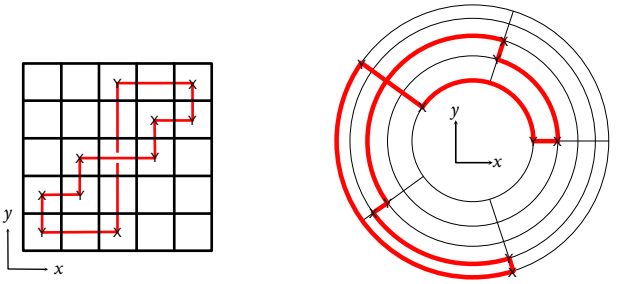

Figure 4. Converting a 5×5 Lagrangian grid diagram to a radial Lagrangian grid diagram.

circles are chosen so that each annular band has area $\frac{\pi}{3n}$ and consequently, each cell, as shown in Figure 4, has equal area (in particular, each cell has area $\frac{1}{n} \cdot \frac{\pi}{3n}$).

For a given marking in row i and column j, we place it in the radial grid at the intersection of the circle C_i with the radial line segment determined by the angle $j\frac{2\pi}{n}$ to obtain a radial grid diagram. Join the markings in the radial grid diagram to match the original grid diagram (see Figure 4).

Remark 3.22. Notice that while the markings of the oriented grid diagram are placed in the cells of the grid, the markings of the radial grid diagram are placed at the intersections of the grid lines. This is just a shift of the markings by $\left(-\frac{1}{2}, -\frac{1}{2}\right)$.

Suppose that $\hat{G}_{x_1y_1}$ and $\hat{G}_{x_2y_2}$ are radial grid diagrams constructed (as above) from Lagrangian grid diagrams $G_{x_1y_1}$ and $G_{x_2y_2}$. We can define an immersion $f : T^2 \to B^2$ by letting $\gamma_1 : \theta_1 \mapsto (x_1(\theta_1), y_1(\theta_1))$ and $\gamma_2 : \theta_2 \mapsto (x_2(\theta_2), y_2(\theta_2))$ be the two loops corresponding to the radial grid diagrams $\hat{G}_{x_1y_1}$ and $\hat{G}_{x_2y_2}$.

We wish to lift f to a Legendrian torus in S^5 using Theorem 2.2, but to do so, it must first be smoothed. This may be remedied by following a smoothing procedure as described in Theorem 3.9, Corollary 3.10, Scholium 3.12, and Corollary 3.13 of [4], and noting that the integral used to define the lift in Theorem 2.2 results in a net area calculation here, just as it was in [4]. To see this, observe that for a path that follows a radial segment in one of the grids, the change in t is 0. For a path that follows a circular arc in one of the grids, the contribution to the change in t is given by ar^2 where a is the subtended angle of the arc (positive if the segment is oriented counterclockwise and negative otherwise), and r is the radius of the arc. That is to say, the magnitude of the change in t along such an arc is twice the area of the sector it bounds (and positive if the arc run counterclockwise, and negative otherwise). Since the radial grid is constructed so that every cell has equal area, the proofs of Theorem 3.9, Corollary 3.10, Scholium 3.12, and Corollary 3.13 in [4] may be easily adapted to this setting. Combining this with Theorem 2.2 we obtain the following:

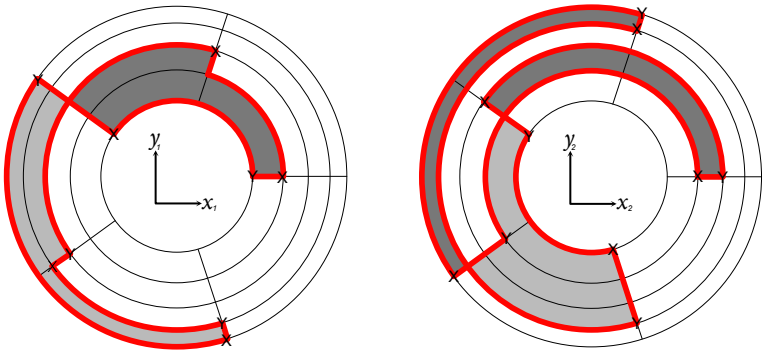

Figure 5. A pair of loops that give rise to a Lagrangian cone.

Theorem 3.23. *Let $\hat{G}_{x_1y_1}$ and $\hat{G}_{x_2y_2}$ be radial grid diagrams constructed from Lagrangian grid diagrams $G_{x_1y_1}$ and $G_{x_2y_2}$, and let $\gamma_1 : \theta_1 \mapsto (x_1(\theta_1), y_1(\theta_1))$ and $\gamma_2 : \theta_2 \mapsto (x_2(\theta_2), y_2(\theta_2))$ be the immersed loops defined by these radial grid diagrams. Then the immersed torus $f : T^2 \to B^2$,*

$$f(\theta_1, \theta_2) = (x_1(\theta_1), y_1(\theta_1), x_2(\theta_2), y_2(\theta_2), \sqrt{1 - x_1^2 - y_1^2 - x_2^2 - y_2^2}, 0),$$

lifts to an immersed Legendrian torus $\tilde{f} : T^2 \to S^5 \subset \mathbb{C}^3$,

$$\tilde{f}(\theta_1, \theta_2) = e^{it(\theta_1, \theta_2)}(x_1(\theta_1), y_1(\theta_1), x_2(\theta_2), y_2(\theta_2), \sqrt{1 - x_1^2 - y_1^2 - x_2^2 - y_2^2}, 0),$$

whose cone in $\mathbb{C}^3$ is Lagrangian.

Consider the example shown in Figure 5. The dark shaded region of the first diagram has area $3 \cdot \frac{\pi}{75}$, as does the light shaded region. However, if we orient the two regions, using the orientation of the knot along the boundary of each, we see that the two regions have opposite orientation. The result of this is that when computing the change in t, the contributions of each region will have opposite sign. Since each contribution is equal in magnitude, the total change in t when traversing the entire knot is 0. Moreover, observe that the difference in the t coordinates at the crossing is $3 \cdot \frac{2\pi}{75}$. Similarly, one can see that the total change in t for the second grid diagram is 0, and that the difference in the t coordinates at each crossing is $2 \cdot \frac{2\pi}{75}$.

Remark 3.24. In general, beginning with two Lagrangian grid diagrams, converting to radial grid diagrams, and lifting, one produces an immersed torus, and hence an immersed Lagrangian cone. To get an embedded torus, and hence an embedded Lagrangian cone, one must check to see that the product lift condition is satisfied by the pair of Lagrangian grid diagrams (see Section 4 of [4]). This amounts to checking that condition (2) of Theorem 2.2 is satisfied. The pair of radial grid diagrams shown in Figure 5 satisfies the product lift condition, as one may check.

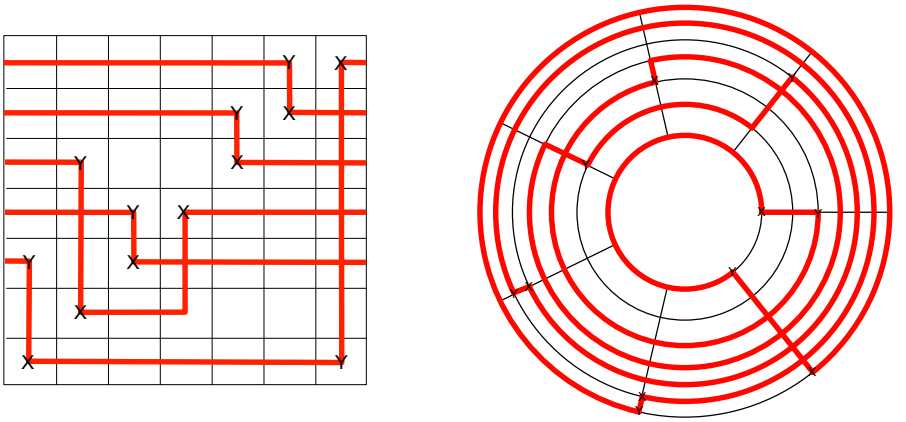

Figure 6. A 7×7 radial Lagrangian grid, with the associated grid diagram from which it is constructed.

Remark 3.25. In Proposition 3.4 of [4] it was shown that the immersion determined by a Lagrangian grid diagram could be smoothed in such a way as to ensure that the lift of the smoothed immersion is C^0-close to the lift of the original immersion, and that any two smoothings, sufficiently close to the original immersion, would have Legendrian isotopic lifts. The proof of that proposition depended only on the fact that the lift was determined by a net-area calculation. Since the same is true in this setting, the proof may be adapted to this situation, to produce a smoothly embedded Lagrangian cone.

The family of examples produced here is specific to the case $n = 3$, but only because the Lagrangian hypercube diagrams are constructed, at this time, only in dimension 4. Yet, it is clear that Lagrangian hypercube diagrams may be generalized to produce Lagrangian immersions $f : T^{n-1} \to B^{n-1}$.

3D. ***Examples constructed from radial hypercube diagrams.*** In the previous example, beginning with a pair of Lagrangian grid diagrams meant that for any loop on the immersed torus in B^2, in the lift, the net change in t is 0. However, this is more restrictive than necessary, since we still obtain a well-defined lift provided that the net change in t along any loop downstairs is an integer multiple of 2π. In fact, we may relax the conditions of the previous example a bit more, as follows.

Let $G_{x_1y_1}$ and $G_{x_2y_2}$ be two grid diagrams, and construct radial grid diagrams $\hat{G}_{x_1y_1}$ and $\hat{G}_{x_2y_2}$ by placing markings as in the previous example. However, to obtain an immersed loop from the diagram, we follow a slightly different procedure. Along each radial column, join the markings as in the original grid diagram. In each circular row, there are two arcs oriented from X to Y. Choose one of the two oriented arcs in each row. Figure 6 shows one example of a grid diagram, with a particular choice of connections made in each row. Thus to a given grid diagram of

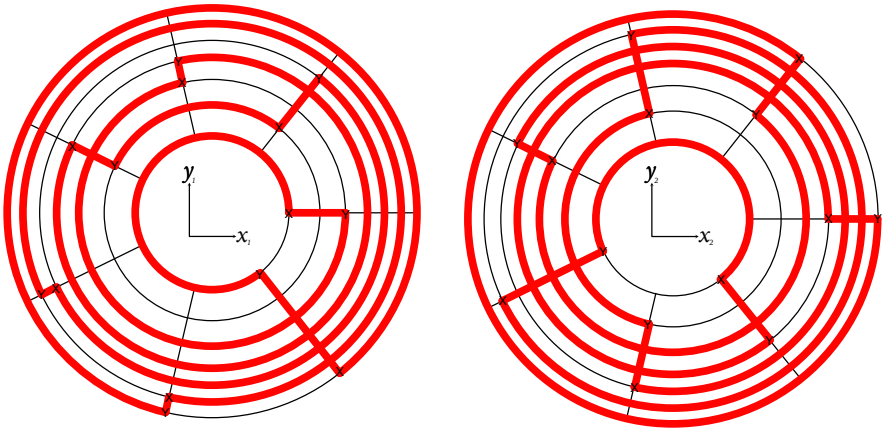

Figure 7. A pair of 7×7 radial grid diagrams that give rise to a Lagrangian cone.

size n, there are 2^n distinct, immersed loops that correspond to it by following this procedure.

Theorem 3.26. *Let $\hat{G}_{x_1y_1}$ and $\hat{G}_{x_2y_2}$ be radial grid diagrams and let*

$$\gamma_1 : \theta_1 \mapsto (x_1(\theta_1), y_1(\theta_1)) \quad \text{and} \quad \gamma_2 : \theta_2 \mapsto (x_2(\theta_2), y_2(\theta_2))$$

be the immersed loops defined by these radial grid diagrams, together with a choice of oriented circular arcs.

Suppose that $\sum_{i=1}^{n} a_i r_i^2 = 2\pi k_1$, where a_i is the angle subtended by the chosen arc in row i of $\hat{G}_{x_1,y_1}$, r_i is the radius of the corresponding circle, and $k_1 \in \mathbb{Z}$. Similarly assume that $\sum_{i=1}^{n} b_i r_i^2 = 2\pi k_2$, where b_i is the angle subtended by the chosen arc in row i of $\hat{G}_{x_2,y_2}$, r_i is the radius of the corresponding circle, and $k_2 \in \mathbb{Z}$. Then the immersed torus $f : T^2 \to B^2$,

$$f(\theta_1, \theta_2) = (x_1(\theta_1), y_1(\theta_1), x_2(\theta_2), y_2(\theta_2), \sqrt{1 - x_1^2 - y_1^2 - x_2^2 - y_2^2}, 0),$$

lifts to an immersed Legendrian torus $\tilde{f} : T^2 \to S^5 \subset \mathbb{C}^3$,

$$\tilde{f}(\theta_1, \theta_2) = e^{it(\theta_1,\theta_2)}(x_1(\theta_1), y_1(\theta_1), x_2(\theta_2), y_2(\theta_2), \sqrt{1 - x_1^2 - y_1^2 - x_2^2 - y_2^2}, 0),$$

where t is defined as in Theorem 2.2, and whose cone in $\mathbb{C}^3$ is Lagrangian.

Proof. The proof follows from Theorem 2.2 together with the observations of Theorem 3.23 that the change in t may be interpreted as a net-area calculation. The condition that $\sum_{i=1}^{n} a_i r_i^2 = 2\pi k_1$ and $\sum_{i=1}^{n} b_i r_i^2 = 2\pi k_2$ guarantees that the net-area of the loops determined by $\hat{G}_{x_1y_1}$ and $\hat{G}_{x_2y_2}$, is a multiple of 2π and hence, each loop lifts to a loop that wraps around the fiber k_1 or k_2 times. □

The two radial grid diagrams shown in Figure 7 determine an immersion that lifts to a torus whose cone is Lagrangian. A net-area calculation shows that the cone is embedded, since the two diagrams satisfy the product lift condition (see Section 4 of [4]). Moreover, the lift has the property that each diagram lifts to a loop that wraps once around the fiber.

Remark 3.27. The pair of grid diagrams chosen at the beginning determine a structure, similar to a hypercube diagram, which we will refer to as a *radial Lagrangian hypercube diagram*.

Remark 3.28. Remark 3.25 applies in this situation as well, allowing us to produce smooth Lagrangian cones using radial Lagrangian hypercube diagrams.

In light of Example 3.1, it is natural to ask which Lagrangian hypercube diagram gives rise to the Harvey–Lawson cone. Note that the immersion given in Example 3.1 does not readily admit the structure of a Lagrangian hypercube diagram. It has only two double point circles, neither of which intersect, while any Lagrangian hypercube diagram must contain double point circles that intersect (since each Lagrangian grid diagram used to define a Lagrangian hypercube diagram must contain crossings, each of which produces a double point circle in the product). Nevertheless, it seems likely that there is a Lagrangian hypercube representation of the Harvey–Lawson cone, hence:

Conjecture 3.29. *There exists a radial Lagrangian hypercube diagram, whose associated Lagrangian cone in $\mathbb{C}^3$ is isotopic to the Harvey–Lawson cone.*

While we do not address the construction of the perturbation of a Lagrangian hypercube diagram needed to ensure that the corresponding torus in $\mathbb{C}P^2$ has only isolated transverse double points, techniques similar to those of Section 3 paired with the techniques described by Peter Lambert-Cole in [16; 17] can be used to do exactly that.

Lastly, while a radial Lagrangian hypercube diagram will not lift to a special Lagrangian cone, it may lift to a Lagrangian cone which is isotopic to a special Lagrangian cone. This leads us to pose the following question:

Question 1. What conditions on a radial Lagrangian hypercube diagram ensure that the Lagrangian cone to which it lifts is isotopic to a special Lagrangian cone? Are there any obstructions?

4. The lifting theorem

While Theorem 2.2 applies only to immersions into a unit ball, $B^{n-1} \subset \mathbb{C}^{n-1}$, thought of as a single chart of $\mathbb{C}P^{n-1}$, it can be generalized to any immersion $f : \Sigma^{n-1} \to \mathbb{C}P^{n-1}$ so that the lifting process works in much the same way as it does in Theorem 2.2. This is the content of the lifting theorem below. We build

up to the lifting theorem through a series of computationally useful lemmas and definitions.

Recall that the symplectic form associated with the Fubini–Study metric is, in coordinates $z = (z_1, \ldots, z_n)$ of $\pi_{\mathbb{C}^*} : \mathbb{C}^n \setminus \{0\} \to \mathbb{C}P^{n-1}$, given by

$$\pi^*_{\mathbb{C}^*}(\omega_{FS}) = \frac{i}{2} \cdot \frac{1}{|z|^4} \sum_{k=1}^{n} \sum_{j \neq k} (\overline{z_j} z_j dz_k \wedge d\overline{z_k} - \overline{z_j} z_k dz_j \wedge d\overline{z_k}). \tag{4-1}$$

The form ω_{FS} is the form induced upon $\mathbb{C}P^{n-1}$ after quotienting by the invariant $\mathbb{C}^*$ action. One can check that

$$\int_{\mathbb{C}P^1} \omega_{FS} = \pi$$

and therefore $\frac{1}{\pi}\omega_{FS}$ is an integral symplectic form on $\mathbb{C}P^{n-1}$. Furthermore, for $i : S^{2n-1} \to \mathbb{C}^n$, it is well known that ω_{FS} is the unique form such that $i^*(\omega_0) = \pi^*(\omega_{FS})$ where $\pi : S^{2n-1} \to \mathbb{C}P^{n-1}$ is the Hopf fibration and ω_0 is the standard symplectic form on $\mathbb{C}^n$, i.e., for $z_i = x_i + iy_i$,

$$\omega_0 = \frac{i}{2} \sum_{i=1}^{n} dz_i \wedge d\overline{z_i} = \sum_{i=1}^{n} dx_i \wedge dy_i.$$

As mentioned above, the usual homogeneous, holomorphic coordinate system on $\mathbb{C}P^{n-1}$ is not suitable for our purposes. Instead, we use the hemispherical coordinate system:

Definition 4.1. Let $B_i \subset \mathbb{C}^{n-1}$ be the open unit ball and define coordinate charts $\psi_i : B_i \to \mathbb{C}P^{n-1}$, $j = 1, \ldots, n$, given by

$$\psi_i(z_1, \ldots, z_{i-1}, z_{i+1}, \ldots, z_n) = [z_1 : \cdots : z_{i-1} : \sqrt{1 - |z|^2} : z_{i+1} : \cdots : z_n].$$

The charts, (B_i, ψ_i) are called *hemispherical charts*.

Note that we are numbering the z_i's in terms of $\mathbb{C}^n$ instead of $\mathbb{C}^{n-1}$. For example, for $n = 3$, $z \in B_2 \subset \mathbb{C}^2$ is defined by $z = (z_1, z_3)$ and is mapped to $\mathbb{C}P^3 = \mathbb{C}^3 \setminus \{0\}/\mathbb{C}^*$ as $\psi_2(z_1, z_3) = \left[z_1 : \sqrt{1 - |z|^2} : z_3\right]$ where $|z|^2 = |z_1|^2 + |z_3|^2$. We will often use the hat symbol to denote removing a term. Hence $z = (z_1, z_3)$ could also be written as $z = (z_1, \hat{z}_2, z_3)$ to simplify notation.

Also, we use U_i to refer to the image of B_i in $\mathbb{C}P^{n-1}$, i.e., $U_i = \psi_i(B_i)$. The name of the system obviously follows from the fact that the image of each chart is the image of a hemisphere in $S^{2n-1} \subset \mathbb{C}^n$ via the Hopf fibration $\pi : S^{2n-1} \to \mathbb{C}P^{n-1}$.

The hemispherical charts ψ_i are not holomorphic with respect to the natural complex structure on $\mathbb{C}P^{n-1}$. However, they do have one very nice property: the ψ_i's are Darboux charts on $\mathbb{C}P^{n-1}$.

Lemma 4.2. *If ω_0 is the standard symplectic form on $B \subset \mathbb{C}^{n-1}$ then*

$$\omega_0 = \psi_i^*(\omega_{FS}).$$

Proof. For $n = 2$, observe that in homogeneous coordinates, (4-1) translates into

$$\tilde{\omega}_{FS} = \frac{i}{2|z|^4}(\overline{z_2}z_2 dz_1 \wedge d\overline{z_1} - \overline{z_2}z_1 dz_2 \wedge d\overline{z_1} + \overline{z_1}z_1 dz_2 \wedge d\overline{z_2} - \overline{z_1}z_2 dz_1 \wedge d\overline{z_2}).$$

Observe that in B_1, $z_1 = \sqrt{1 - |z_2|^2}$. Using this observation, and changing to real coordinates, observe that in hemispherical coordinates, $\tilde{\omega}_{FS} = dx_2 \wedge dy_2$, which is ω_0 in the chart B_1. The general calculation is similar. □

Before moving on, we can characterize the sets U_i and point out that the ψ_i's are a chart system (all points of $\mathbb{C}P^{n-1}$ are in at least one chart). Let $[z_1 : \cdots : z_n] \in \mathbb{C}P^{n-1}$. At least one coordinate is nonzero, say $z_i \neq 0$. In the preimage of the quotient map for $\mathbb{C}P^{n-1} = (\mathbb{C}^n \setminus 0)/\mathbb{C}^*$, the point $(z_1, \ldots, z_n)$ is equivalent to

$$\frac{\overline{z_i}}{|z_i||z|}(z_1, \ldots, z_n)$$

where $|z| = \sqrt{|z_1|^2 + \cdots + |z_n|^2}$. Therefore $[z_1 : \cdots : z_n] \in U_i$ and

$$U_i = \{[z_1 : \cdots : z_n] \mid z_i \neq 0\}.$$

Thus, the hemispherical chart system allows us to work with $f(\Sigma)|_{U_i} \subset B_i$ using the standard symplectic form ω_0.

Hemispherical charts also trivialize the Hopf fibration over $\mathbb{C}P^{n-1}$. In the diagram

$$\begin{array}{ccccc} B_i \times S^1 & \xrightarrow{\Psi_i} & S^{2n-1} & \hookrightarrow & \mathbb{C}^n \\ \downarrow{\scriptstyle \pi} & & \downarrow{\scriptstyle \pi_{S^1}} & & \\ B_i & \xrightarrow{\psi_i} & \mathbb{C}P^{n-1} & & \end{array}$$

$B_i \times S^1$ is a trivialization of the S^1-bundle, $\pi : S^{2n-1} \to \mathbb{C}P^{n-1}$, given by

$$\Psi_i(z, e^{it}) = e^{it}(z_1, \ldots, z_{i-1}, \sqrt{1 - |z|^2}, z_{i+1}, \ldots, z_n) \in S^{2n-1} \subset \mathbb{C}^n.$$

The diagram commutes and Ψ_i gives a trivialization of the Hopf fibration over $U_i \subset \mathbb{C}P^{n-1}$.

As mentioned before, there is a natural contact form α on the unit sphere S^{2n-1} in $\mathbb{C}^n$. Given $z = (z_1, \ldots, z_n) \in \mathbb{C}^n$ where $z_i = x_i + iy_i$ and $\omega_0 = \frac{i}{2}\sum_{i=1}^n dz_i \wedge d\overline{z_i} = \sum_{i=1}^n dx_i \wedge dy_i$, the form on $\mathbb{C}^n$,

$$\alpha_0 = \frac{1}{2}\left(\sum_{i=1}^n x_i dy_i - y_i dx_i\right),$$

is a contact form when restricted to S^{2n-1}. Set $\alpha = \alpha_0|_{S^{2n-1}}$. Equipped with this contact form, (S^{2n-1}, α) is a contact manifold.

We collect a few facts about α, partly to set notation for the reader, and partly to justify choices and conventions used throughout this paper.

Lemma 4.3. *For $z = (z_1, \ldots, z_n) \in \mathbb{C}^n \setminus 0$ where $z_i = x_i + iy_i$, let*

$$N_z = x_1 \frac{\partial}{\partial x_1} + y_1 \frac{\partial}{\partial y_1} + \cdots + x_n \frac{\partial}{\partial x_n} + y_n \frac{\partial}{\partial y_n}$$

be the outward pointing normal vector field for any sphere of radius $r > 0$, centered at the origin in $\mathbb{R}^{2n}$, and

$$T_z = x_1 \frac{\partial}{\partial y_1} - y_1 \frac{\partial}{\partial x_1} + \cdots + x_n \frac{\partial}{\partial y_n} - y_n \frac{\partial}{\partial x_n}$$

be the vector field that generates the Hopf fibration $\pi : S^{2n-1} \to \mathbb{C}P^{n-1}$. Then the following are facts about α_0 and the contact form α:

(1) *The form α_0 is equal to $\iota_{\frac{1}{2}N_z}\omega_0$ when $|z| = 1$.*

(2) *The form α_0 also satisfies $\alpha_0(kT_z) = \frac{k}{2}|z|^2$ for k a constant, and $\iota_{T_z} d\alpha_0 = \iota_{T_z}\omega_0 = -\sum_{i=1}^{n}(x_i dx_i + y_i dy_i)$. For any vector $v \in T_z S_r^{2n-1}$ for a sphere of radius $r = |z|$,*

$$\iota_{T_z} d\alpha_0(v) = -\langle N_z, v\rangle = 0,$$

where $\langle\ ,\ \rangle$ is the usual inner product on $\mathbb{R}^{2n}$. Therefore the vector field R, defined by $R = 2T_z$ when restricted to $|z| = 1$, is the Reeb vector field of α, i.e., $\alpha(R) = 1$ and $d\alpha(R, \cdot) = 0$.

(3) *Since $i^*(\omega_0) = \pi^*(\omega_{FS})$ and $d\alpha_0 = \omega_0$, $\frac{i}{\pi}\alpha$ is the connection one-form of the integral cohomology class $\left[\frac{1}{\pi}\omega_{FS}\right]$.*

We use α for η in Theorem 2.1 to find $\Psi_i^*(\alpha)$ in the trivialization $B_i \times S^1$ with coordinates (z, e^{it}).

Lemma 4.4. *Let $B_j \subset \mathbb{C}^{n-1}$ be the unit ball with coordinates*

$$z = (z_1, \ldots, z_{j-1}, z_{j+1}, \ldots, z_n).$$

For a chart $\psi_j : B_j \to \mathbb{C}P^{n-1}$ and trivialization $\Psi_j : B_j \times S^1 \to S^{2n-1}$ given by $\Psi_j(z, e^{it}) = e^{it}(z_1, \ldots, z_{j-1}, \sqrt{1 - |z|^2}, z_{j-1}, \ldots, z_n)$,

$$\Psi_j^*(\alpha) = \tfrac{1}{2}(dt + 2\alpha_0),$$

where α_0 is the form defined above on $B_j \subset \mathbb{C}^{n-1}$.

In polar coordinates,

$$\Psi_j^*(\alpha) = \tfrac{1}{2}\big(dt + r_1^2 d\theta_1 + \cdots + \widehat{r_j^2 d\theta_j} + \cdots + r_n^2 d\theta_j\big).$$

Note that the α_0 defined on B_j has no z_j term of the form $(x_j dy_j - y_j dx_j)$ since $z \in B_j$ has coordinates $z = (z_1, \ldots, \hat{z_j}, \ldots, z_n)$. The proof of the lemma is a calculation, and left to the reader.

Thus we can take τ in Theorem 2.1 to be the 1-form $-2\alpha_0 \in \Omega^1(B_j)$. In each chart $B_j \times S^1$, label $\tau_j = -2\alpha_0$; note that the transition map $\Psi_{kj} : B_j \times S^1 \to B_k \times S^1$ takes

$$\Psi_{kj}^*\big(\tfrac{1}{2}(dt - \tau_k)\big) = \tfrac{1}{2}(dt - \tau_j). \tag{4-2}$$

This result follows from the next lemma.

Lemma 4.5. *Let B_j be the unit ball in $\mathbb{C}^{n-1}$ with coordinates*

$$z = (z_1, \ldots, z_{j-1}, z_{j+1}, \ldots, z_n),$$

and let the function $\Psi_j : B_j \times S^1 \to S^{2n-1} \subset \mathbb{C}^n$ be given by $\Psi_j(z, e^{it}) = e^{it}(z_1, \ldots, z_{j-1}, \sqrt{1-|z|^2}, z_{j+1}, \ldots, z_n)$ where $|z| = |z_1|^2 + \cdots + \widehat{|z_j|^2} + \cdots + |z_n|^2$. For $k \neq j$, the map

$$\Psi_{kj} : B_j \setminus \{z_k = 0\} \times S^1 \to B_k \setminus \{z_j = 0\} \times S^1$$

defined by $\Psi_{kj} = \Psi_k^{-1} \circ \Psi_j$ is given by the map

$$\begin{aligned}
&\Psi_{kj}(z, e^{it}) \\
&\quad = \Bigg(z_1 \frac{\overline{z_k}}{|z_k|}, \ldots, z_{k-1}\frac{\overline{z_k}}{|z_k|}, |z_k|, z_{k+1}\frac{\overline{z_k}}{|z_k|}, \\
&\qquad\qquad \ldots, z_{j-1}\frac{\overline{z_k}}{|z_k|}, \frac{\overline{z_k}}{|z_k|}\sqrt{1-|z|^2}, z_{j+1}\frac{\overline{z_k}}{|z_k|}, \ldots, z_n\frac{\overline{z_k}}{|z_k|}, e^{it}\frac{z_k}{|z_k|} \Bigg)
\end{aligned}$$

In polar coordinates,

$$\begin{aligned}
&\Psi_{kj}(r_1, \theta_1, \ldots, \hat{r_j}, \hat{\theta_j}, \ldots, r_n, \theta_n, t) = \\
&\qquad \Bigg(r_1, \theta_1 - \theta_k, r_2, \theta_2 - \theta_k, \ldots, r_{j-1}, \theta_{j-1} - \theta_k, \sqrt{1 - \textstyle\sum_{i=1, i\neq j}^{n} r_i^2}, \\
&\qquad\qquad -\theta_k, r_{j+1}, \theta_{j+1} - \theta_k, \ldots, r_n, \theta_n - \theta_k, t + \theta_k \Bigg)
\end{aligned}$$

Proof. We show the calculation for B_2, $B_3 \subset \mathbb{C}^3$. The general case is similar. The maps

$$\Psi_2 : B_2 \times S^1 \to S^7 \subset \mathbb{C}^4,$$

$$\Psi_2(z_1, z_3, z_4, e^{it}) = e^{it}(z_1, \sqrt{1-|z|^2}, z_3, z_4),$$

and

$$\Psi_3 : B_3 \times S^1 \to S^7 \subset \mathbb{C}^4,$$

$$\Psi_3(w_1, w_2, w_4, e^{it}) = e^{it}(w_1, w_2, \sqrt{1-|w|^2}, w_4)$$

give rise to $\Psi_{32} : B_2 \setminus \{z_3 = 0\} \times S^1 \to B_3 \setminus \{w_2 = 0\} \times S^1$ via $\Psi_3^{-1} \circ \Psi_2$. By

multiplying by 1 appropriately,

$$\begin{aligned}
&\Psi_2(z_1, z_3, z_4, e^{it}) \\
&\qquad = e^{it}\big(z_1, \sqrt{1-|z_1|^2-|z_3|^2-|z_4|^2}, z_3, z_4\big) \\
&\qquad = e^{it}\left(\frac{z_3}{|z_3|}\frac{\overline{z_3}}{|z_3|}\right)\big(z_1, \sqrt{1-|z_1|^2-|z_3|^2-|z_4|^2}, z_3, z_4\big) \\
&\qquad = e^{it}\left(\frac{z_3}{|z_3|}\right)\left(z_1\frac{\overline{z_3}}{|z_3|}, \frac{\overline{z_3}}{|z_3|}\sqrt{1-|z_1|^2-|z_3|^2-|z_4|^2}, z_3\frac{\overline{z_3}}{|z_3|}, z_4\frac{\overline{z_3}}{|z_3|}\right) \\
&\qquad = \Psi_3(w_1, w_2, w_4, e^{it'})
\end{aligned}$$

where $w_1 = z_1\,\overline{z_3}/|z_3|$, $w_2 = \overline{z_3}/|z_3|\,\sqrt{1-|z|^2}$, $w_4 = z_4\,\overline{z_3}/|z_3|$, and $e^{it'} = e^{it}z_3/|z_3|$. One can check that $(w_1, w_2, w_4, e^{it}) \in B_3 \setminus \{w_2 = 0\}$ and $e^{it}z_3/|z_3| \in S^1$ and $\sqrt{1-|w_1|^2-|w_2|^2-|w_4|^2} = |z_3|$ as desired. □

Remark 4.6. The formula for Ψ_{kj} also gives the formula for $\psi_{kj} : B_j \setminus \{z_k = 0\} \to B_k \setminus \{z_j = 0\}$ for $\psi_{kj} = \psi_k^{-1} \circ \psi_j$ by looking at the z coordinates of (z, e^{it}).

In summary, given a Lagrangian immersion $f : \Sigma \to \mathbb{C}P^{n-1}$ and $V_j = f(\Sigma) \cap B_j$, we can work with $V_j \subset B_j$ using

- the standard symplectic form ω_0 on $B_j \subset \mathbb{C}^{n-1}$,
- the standard 1-form $\tau_j = -2\alpha_0$ on $B_j \subset \mathbb{C}^{n-1}$,

and patch the V_j's together using the transition maps $\psi_{kj} : B_j \to B_k$ given by $\psi_{kj} = \psi_k^{-1} \circ \psi_j$.

In practice, this allows us to do integration and other calculations in the B_j's using standard forms in each instead of working with homogeneous coordinates and ω_{FS} in $\mathbb{C}P^{n-1}$.

This chart system also gives us new ways to build examples of Lagrangian immersions by first working with piecewise linear submanifolds in each ball B_j, pasting the pieces together, and then smoothing the result (as is done with Lagrangian hypercubes in [2] and Section 3 of [4]).

4A. ***The lifting theorem.*** The lifting theorem puts the separate pieces in the previous sections together into one result. First, we need an explicit way to calculate integrals along paths in $f(\Sigma)$.

Let $f : \Sigma \to \mathbb{C}P^{n-1}$ be a Lagrangian immersion and let $\gamma : I \to \Sigma$ be a path. In order to define the lift, we need to define a map $t : I \to \mathbb{R}/2\pi\mathbb{Z}$, which we do in pieces. Split the interval I into subintervals

$$I = \bigcup_{k=0}^{m-1} [s_k, s_{k+1}]$$

where $0 = s_0 < s_1 < \cdots < s_{m-1} < s_m = 1$ such that $f(\gamma([s_k, s_{k+1}])) \subset B_j$ for

some $j \in \{1, \dots, n\}$ (after identifying B_j with U_j using ψ_j). Index the B_j's by j_k so that $f(\gamma([s_k, s_{k+1}])) \subset B_{j_k}$ where j_k is the index of the chart in which $\gamma([s_k, s_{k+1}])$ is contained. Let $x_k = \gamma(s_k)$ so that $x_0 = \gamma(s_0)$ and $x_m = \gamma(s_m)$. Also, for convenience, use the notation $(z)_k$ to stand for the z_k coordinate of $z \in B_j$. (If $z \in B_3 \subset \mathbb{C}^3$ such that $z = (z_1, z_2, z_4)$ then $(z)_4 = z_4$.)

Since $f(\gamma([s_0, s_1])) \subset B_{j_0}$, we can integrate $\tau_{j_0} = -2\alpha_0$ (see (4-2)) along the path $f(\gamma([s_0, s_1]))$. Define $t_0 : [s_0, s_1] \to \mathbb{R}/2\pi\mathbb{Z}$ by

$$t_0(s) = \left(\int_0^s \tau_{j_0}((f \circ \gamma)'(u))\, du \right) \bmod 2\pi,$$

where $t_0(0) = 0$.

For $s \in [s_0, s_1]$ and $t(0) = a$, we can write

$$t(s) = t_0(s) + a.$$

The point $(f(\gamma(s_1)), e^{it(s_1)}) \in B_{j_0} \times S^1$ also lives as a point $\Psi_{j_1 j_0}(f(\gamma(s_1)), e^{it(s_1)}) \in B_{j_1} \times S^1$. Define $\Psi_{j_1 j_0}(t(s_1)) \in \mathbb{R}/2\pi\mathbb{R}$ to be the argument of the S^1 component of this map in $B_{j_1} \times S^1$. We can also define the point $\psi_{j_1 j_0}(f(\gamma(s_1)) \in B_{j_1}$ as the B_{j_1} component of $B_{j_1} \times S^1$ (see Remark 4.6).

Lemma 4.7. *When $t(s_k)$ is defined for $(f(\gamma(s_k)), e^{it(s_k)}) \in B_{j_{k-1}}$, then $\Psi_{j_k j_{k-1}}(t(s_k)) = t(s_k) + arg(\psi_{j_k j_{k-1}}(f(\gamma(s_k)))_{j_k})$.*

Proof. See Lemma 4.5. □

We can now continue the integration in B_{j_1}: Define $t_1 : [s_1, s_2] \to \mathbb{R}/2\pi\mathbb{Z}$ by $t_1(s_1) = 0$ and

$$t_1(s) = \left(\int_{s_1}^s \tau_{j_1}((f \circ \gamma)'(u))\, du \right) \bmod 2\pi.$$

Hence we can write $t(s)$ for $s \in [s_1, s_2]$ as

$$t(s) = t_1(s) + \Psi_{j_1 j_0}(t_0(s_1) + a).$$

Induct on k to integrate the τ_{j_k}'s over the entire path:

Definition 4.8. Let $[0, 1] \xrightarrow{\gamma} \Sigma \xrightarrow{f} \mathbb{C}P^{n-1}$ and suppose there exists an increasing sequence $0 = s_0 < s_1 < \cdots < s_{m-1} < s_m = 1$ such that $f(\gamma([s_k, s_{k+1}])) \subset B_{j_k}$ for $j_k \in \{1, \dots, n\}$ and $f(\gamma(s_k)) \neq 0$ and $f(\gamma(s_{k+1})) \neq 0$ for all $0 \leq k \leq m$. Assume $t(0) = a$ and define the *lifting integral* to be

$$\Gamma \int_\gamma \tau := \Big[t_{m-1}(s_m) + \Psi_{j_{m-1} j_{m-2}}\big(\cdots\big(t_3(s_4) + \Psi_{j_3 j_2}\big(t_2(s_3) + \Psi_{j_2 j_1}\big(t_1(s_2) + \Psi_{j_1 j_0}(t_0(s_1) + a)\big)\big)\big)\big)\Big] \bmod 2\pi.$$

Remark 4.9. See Example 5.1 for an example of a calculation of the lifting integral for the trivial cone.

In practice we usually need only $m = 1$ or $m = 2$ for most integrals. Also, since

$$\tau_{j_k} = -\sum_{i=1,\, i\neq j_k}^{n} (x_i dy_i - y_i dx_i) \quad \text{and} \quad \omega_{FS}|_{B_{j_k}} = \sum_{i=1,\, i\neq j}^{n} dx_i \wedge dy_i,$$

the calculations may be done in each chart. In summary, we obtain the lifting theorem, which says that if

(1) $\Gamma \int_\gamma \tau = 0 \bmod 2\pi$ for all $[\gamma] \in H_1(\Sigma; \mathbb{Z})$, and

(2) for all distinct points $x_1, \ldots, x_k \in \Sigma$ such that $f(x_1) = f(x_j)$ for all $j \leq k$, and a choice of path γ_j from x_1 to x_j in Σ for $2 \leq j \leq k$, the set

$$\left\{ \left(\Gamma \int_{f(\gamma_j)} \tau \right) \bmod 2\pi \mid 2 \leq j \leq k \right\}$$

has $k-1$ distinct values, none of which are equal to 0,

then $f : \Sigma \to \mathbb{C}P^{n-1}$ lifts to an embedding $\tilde{f} : \Sigma \to S^{2n-1}$ such that the image (the lift) $\tilde{\Sigma}$ is a Legendrian submanifold of (S^{2n-1}, α). Furthermore, the cone $c\tilde{\Sigma}$ is Lagrangian in $\mathbb{C}^n$ with respect to the standard symplectic structure ω_0.

5. Legendrian contact homology generators of the trivial Lagrangian cone

Example 5.1. We already saw in Example 1.6 how to obtain a trivial (special) Lagrangian cone, but, we can also construct this example using the lifting theorem, as a lift of a map $f : S^{n-1} \to \mathbb{C}P^{n-1}$.

Recall that the trivial cone is given by the map $\tilde{f} : \mathbb{R}^n \to \mathbb{C}^n$ where $(x_1, \ldots, x_n) \mapsto (x_1\eta_1, \ldots, x_n\eta_n)$, and $\eta = (\eta_1, \ldots, \eta_n)$ is a complex vector with $\eta_j \neq 0$ for all j. Clearly the trivial cone is a lift of the Lagrangian immersion $f : S^{n-1} \to \mathbb{C}P^{n-1}$ given by $f(x_1, \ldots, x_n) = [x_1\eta_1 : \cdots : x_n\eta_n]$.

Observe that the set $\{(x_1, \ldots, x_n) \subset \mathbb{R}^n \mid \sum_{k=1}^n |x_k\eta_{k,j}|^2 = 1\}$ is an $(n-1)$-dimensional sphere, S^{n-1}, for any choice of complex vector $(\eta_{1,j}, \ldots, \eta_{n,j})$ (the reason for the j-subscript will be apparent shortly). Moreover, we may cover S^{n-1} by charts of the form $\phi_j^{\pm} : V_j^{\pm} \to S^{n-1}$ where $V_j^{\pm} = \left\{(x_1, \ldots, x_{j-1}, \hat{x_j}, x_{j+1}, \ldots, x_n) \in \mathbb{R}^{n-1} \mid \sum_{k=1,\, k\neq j}^n |x_j\eta_{k,j}|^2 < 1\right\}$, and the sign indicates which hemisphere is being covered. Within each chart, after identifying $V_j^{\pm}$ with $\phi_j^{\pm}(V_j^{\pm})$, we may write $f(x)$ as $f_j^{\pm}(x)$ where $f_j^{\pm} : V_j^{\pm} \to \mathbb{C}P^{n-1}$ is given by

$$f_j^{\pm}(x_1, \ldots, x_{j-1}, \hat{x_j}, x_{j+1}, \ldots, x_n) =$$
$$\left[x_1\eta_{1,j} : \cdots : x_{j-1}\eta_{j-1,j} : \pm \sqrt{1 - \sum_{k=1,\, k\neq j}^n |x_k\eta_{k,j}|^2} : x_{j+1}\eta_{j+1,j} : \cdots : x_n\eta_{n,j} \right],$$

where $\eta_{k,j} = \eta_k \overline{x_j\eta_j}/|x_j\eta_j|$.

Since $H_1(S^2, \mathbb{Z})$ is trivial, the first condition of the lifting theorem is automatically satisfied. Moreover, $f_i^{\pm}$ is clearly an embedding on $V_i^{\pm}$, so within each chart the second condition is satisfied. However, observe that after patching these maps together, the antipodal points of S^{n-1} are the only ones identified by f (in fact, the image of f is a copy of $\mathbb{R}P^{n-1}$). To see that the antipodal points are separated in the lift, consider what happens when $n = 3$ and $\eta = (1, 1, 1)$. In that case, we can lift along a path γ from the origin of V_3^+ (the "north pole") to the origin of V_3^- (the "south pole"), and running diametrically through the origin of V_1^+. Notice that integrating τ along γ contributes 0 to the lift within each chart. If we transition from V_3^+ to V_1^+ at the point $(1/\sqrt{2}, 0, 1/\sqrt{2})$ and from V_1^+ to V_3^- at the point $(1/\sqrt{2}, 0, -1/\sqrt{2})$ then we pick up a factor of -1, or $e^{i\pi}$, on the S^1-factor from the transition map Ψ_{31} (the second transition map). Hence,

$$\Gamma \int_\gamma \tau = \pi.$$

The general calculation is similar. Hence, the lifting theorem guarantees the existence of an embedded lift, $\tilde{f} : S^{n-1} \to S^{2n-1} \subset \mathbb{C}^n$ such that the cone is Lagrangian in $\mathbb{C}^n$. Moreover, our discussion above clearly identifies this as a Lagrangian $\mathbb{R}^n \subset \mathbb{C}^n$, which is the trivial cone.

The trivial cone intersects S^{2n-1} in a Legendrian $(n-1)$-sphere that projects down to a copy of $\mathbb{R}P^{n-1}$ via a 2-to-1 map (the quotient by the antipodal map). This is inconvenient when one wishes to compute Legendrian contact homology, because one needs isolated transverse double points. However, we can perturb f through a family of functions f_ϵ so that for some ϵ the image of the lift, $\tilde{f}_\epsilon$, is a copy of S^{n-1} having only transverse double points when projected down to $\mathbb{C}P^{n-1}$.

For simplicity, we write down the perturbation in the case where $n = 3$ and $\eta = (1, 1, 1)$. Choose $\epsilon \geq 0$ and perturb each hemisphere of S^2 as follows:

$$f_{1,\epsilon}^{\pm}(x_2, x_3) = \left[\pm e^{\pm i\epsilon\sqrt{1-x_2^2-x_3^2}}\sqrt{1-x_2^2-x_3^2} : e^{i\epsilon x_2}x_2 : e^{i\epsilon x_3}x_3\right],$$
$$f_{2,\epsilon}^{\pm}(x_1, x_3) = \left[e^{i\epsilon x_1}x_1 : \pm e^{\pm i\epsilon\sqrt{1-x_1^2-x_3^2}}\sqrt{1-x_1^2-x_3^2} : e^{i\epsilon x_3}x_3\right],$$
$$f_{3,\epsilon}^{\pm}(x_1, x_2) = \left[e^{i\epsilon x_1}x_1 : e^{i\epsilon x_2}x_2 : \pm e^{\pm i\epsilon\sqrt{1-x_1^2-x_2^2}}\sqrt{1-x_1^2-x_2^2}\right].$$

Observe that the perturbations in each chart are consistent with the transition maps. To determine the (transverse) intersections, and hence the Reeb chords, we begin with the observation that all double points are antipodal points. We leave the proof as an exercise for the reader.

Theorem 5.2. *Let $f_\epsilon : S^2 \to \mathbb{C}P^2$ be the map determined by patching together $f_{i,\epsilon}^{\pm} : V_i^{\pm} \to \mathbb{C}P^2$ for $i = 1, 2, 3$. Let $(x_1, x_2, x_3), (y_1, y_2, y_3) \in S^2 \subset \mathbb{R}^3$ be two points such that $f_\epsilon(x_1, x_2, x_3) = f_\epsilon(y_1, y_2, y_3)$. Then $(x_1, x_2, x_3) = -(y_1, y_2, y_3)$.*

To determine the double points when $\epsilon > 0$, assume $\pm(x_1, x_2, x_3)$ map to a double point, $f_\epsilon(x_1, x_2, x_3)$. If $x_i \neq 0$ for all i, then without loss of generality we may assume $x_1 > 0$. Using the charts V_1^+ and V_1^-, we see that $f_{1,\epsilon}^+(x_2, x_3) = f_{1,\epsilon}^-(-x_2, -x_3)$, and hence

$$\left[e^{i\epsilon\sqrt{1-x_2^2-x_3^2}}\sqrt{1-x_2^2-x_3^2} : e^{i\epsilon x_2}x_2 : e^{i\epsilon x_3}x_3\right] = \left[-e^{-i\epsilon\sqrt{1-x_2^2-x_3^2}}\sqrt{1-x_2^2-x_3^2} : -e^{-i\epsilon x_2}x_2 : -e^{-i\epsilon x_3}x_3\right]. \quad (5\text{-}1)$$

Cross-multiplying in the first two homogeneous coordinates, we see that

$$e^{i\epsilon(x_2-\sqrt{1-x_2^2-x_3^2})}\sqrt{1-x_2^2-x_3^2} = e^{i\epsilon(-x_2+\sqrt{1-x_2^2-x_3^2})}\sqrt{1-x_2^2-x_3^2}.$$

If $1-x_2^2-x_3^2 \neq 0$, then for small ϵ we may equate the arguments of the exponentials, to obtain $x_2 > 0$ and $2x_2^2 + x_3^2 = 1$. Similarly, cross-multiplying in the first and third homogeneous coordinates, and applying the same reasoning, we obtain $x_3 > 0$ and $x_2^2 + 2x_3^2 = 1$. Solving this system, and recalling that $x_1 = \sqrt{1-x_2^2-x_3^2}$, we obtain that $x_1 = x_2 = x_3 = \pm 1/\sqrt{3}$.

If $1-x_2^2-x_3^2 = 0$ and $x_2 = 0$ then we get a double point at $[0:0:1]$. Similarly, if $1-x_2^2-x_3^2 = 0$ and $x_3 = 0$ then we get a double point at $[0:1:0]$. Finally, assume $x_1 = 0$ and neither x_2 nor x_3 is zero. In this case, working in the charts V_3^+ and V_3^- we obtain

$$\left[0 : e^{i\epsilon x_2}x_2 : e^{i\epsilon\sqrt{1-x_2^2}}\sqrt{1-x_2^2}\right] = \left[0 : -e^{-i\epsilon x_2}x_2 : -e^{-i\epsilon\sqrt{1-x_2^2}}\sqrt{1-x_2^2}\right].$$

For small ϵ, we may use techniques similar to the previous case to obtain that $x_2 = x_3 = \pm\frac{1}{\sqrt{2}}$. A similar discussion applies if $1-x_1^2-x_2^2 = 0$ or $1-x_1^2-x_3^2 = 0$.

From the discussion above, we obtain the following theorem.

Theorem 5.3. *Let $S \subset S^5$ be the Legendrian 2-sphere obtained from intersecting the trivial cone with S^5 and then perturbing it via Legendrian isotopy to the image of $f_{i,\epsilon}^{\pm}$ for $i \in \{1,2,3\}$, for some $\epsilon > 0$. The projection $\pi : S^5 \to \mathbb{C}P^2$ has 7 transverse double points*: $\pm(1,0,0)$, $\pm(0,1,0)$, $\pm(0,0,1)$, $\pm\big(1/\sqrt{2}, 1/\sqrt{2}, 0\big)$, $\pm\big(1/\sqrt{2}, 0, 1/\sqrt{2}\big)$, $\pm\big(0, 1/\sqrt{2}, 1/\sqrt{2}\big)$, *and* $\pm\big(1/\sqrt{3}, 1/\sqrt{3}, 1/\sqrt{3}\big)$. *Then the 0-filtration level of the Legendrian contact homology of S is generated by 7 pairs of short Reeb chords.*

In summary, we have constructed a family of Lagrangian cones, all isotopic to the trivial cone. However, for small $\epsilon > 0$ our cones have the additional property that the projection to $\mathbb{C}P^2$ has 7 transverse double points, while the trivial cone (obtained by taking $\epsilon = 0$) is a 2-to-1 cover of its projection to $\mathbb{C}P^2$.

6. Legendrian submanifolds of S^{2n-1} as lifts of Lagrangian submanifolds in $\mathbb{C}P^{n-1}$

The motivation of this paper is the study of Lagrangian cones given by lifting an immersion into $\mathbb{C}P^{n-1}$ to an embedded Legendrian submanifold of S^{2n-1}. However, Theorem 2.2 and the lifting theorem provide a way to study Legendrian submanifolds of S^{2n-1} on their own.

A lot of work has been done to study Legendrian knots in dimension 3, especially in the standard contact $\mathbb{R}^3$ (see [11; 20; 21; 22; 23; 28]), and Joshua Sabloff studied the Legendrian contact homology of knots in 3-dimensional circle bundles in [30].

Less is known about Legendrian submanifolds in higher dimensions, and much of it only in the standard contact $\mathbb{R}^{2n+1}$ (see [4; 8; 9; 10]). In [29], Legendrian submanifolds of circle bundles over orbifolds are considered, and in [1], the circle bundle $\mathbb{R}^4 \times S^1$ is considered in depth, and related to the case where $\mathbb{R}^4 \times S^1$ is identified with the Hopf bundle over a single chart of $\mathbb{C}P^2$ (the special case of Theorem 2.2 in this paper).

Theorem 2.2 allows one to study Legendrian submanifolds of S^{2n-1} just as one might study Legendrian submanifolds of $\mathbb{R}^{2n} \times S^1$ or even the standard contact $\mathbb{R}^{2n+1}$. As seen in Example 3.1, and Section 3C, the lifts function in much the same way as one might lift an exact Lagrangian to a Legendrian knot in the standard contact $\mathbb{R}^{2n+1}$, or the 1-jet space of a manifold.

Although Theorem 2.2 makes calculations simple, it fails to capture one of the most basic examples: the Legendrian sphere corresponding to the intersection of the trivial cone with S^{2n-1} (as observed in Example 5.1). The lifting theorem moves the story forward, allowing one to consider immersions into $\mathbb{C}P^{n-1}$ that do not lie in a single chart. It shows that the calculations are not much more difficult than they are in the case of Theorem 2.2, because in each chart the calculations use standard forms, and one need only to track how the lifting parameter t transitions from one chart to the next. This leads us to ask the following question:

Question 2. Sabloff showed in [30] how to compute the DGA of Legendrian knots in certain contact circle bundles over surfaces. In the context of Theorem 2.2 or the lifting theorem, is there a similar combinatorial algorithm for computing the Legendrian contact homology in higher dimensional circle bundles?

If such an algorithm can be found, one would expect the structure of a radial Lagrangian hypercube diagram to provide a setting in which such calculations would be simple, and could be automated on a computer.

7. Minimal and Hamiltonian Submanifolds

Special Lagrangian submanifolds, introduced by Harvey and Lawson in [13] have been studied extensively due to their connection with mirror symmetry. Special

Lagrangian cones in $\mathbb{C}^n$ can be studied via the equations that define in them in $\mathbb{C}^n$, as minimal Legendrians in S^{2n-1} (the link), or from the perspective of the corresponding minimal Lagrangian submanifold of $\mathbb{C}P^{n-1}$ (see [14] and [15]). While many examples have been studied, the difficulty in working with the special Lagrangian conditions has led to some weaker conditions being studied in the hope of better understanding special Lagrangians. In [26], the notion of Hamiltonian minimal (H-minimal) Lagrangian submanifolds was introduced. A Lagrangian submanifold in a Kähler manifold is said to be H-minimal if the volume is stationary under compactly supported smooth Hamiltonian deformations (see [15]).

H-minimal Lagrangian cones in $\mathbb{C}^2$ were studied and classified by Schoen and Wolfson in [31]. In particular they showed that only cones of Maslov index ± 1 are area minimizing. Moreover, they showed that if an immersed Lagrangian submanifold of a Kähler–Einstein manifold is stationary for volume, it is automatically minimal, and special Lagrangian in the Calabi–Yau case (see Lemma 8.2 of [31]).

It is already known that the trivial cone is H-minimal (see [18], [24], and [25]). The Harvey–Lawson cone is also known to be strictly Hamiltonian stable, that is, the second variation of the volume is nonnegative under every Hamiltonian deformation, (see [6] and [18]), and it is known that any Hamiltonian stable, minimal Lagrangian torus in $\mathbb{C}P^2$ is congruent to the Clifford torus (see [26], [27] and [33]).

Question 3. What are the conditions on a Lagrangian immersion into $\mathbb{C}P^{n-1}$ that guarantee it lifts to an H-minimal Lagrangian cone?

Question 4. What are the conditions on Legendrian hypercube diagrams that generate H-minimal Lagrangian cones?

References

[1] J. Asplund, *Contact homology of Legendrian knots in five-dimensional circle bundles*, Masters thesis, Uppsala University, 2016, available at https://tinyurl.com/asplund-masters.

[2] S. Baldridge, "Embedded and Lagrangian knotted tori in $\mathbb{R}^4$ and hypercube homology", 2010. arXiv 1010.3742

[3] S. Baldridge and A. M. Lowrance, "Cube diagrams and 3-dimensional Reidemeister-like moves for knots", *J. Knot Theory Ramifications* **21**:5 (2012), 1250033, 39. MR Zbl

[4] S. Baldridge and B. McCarty, "On the rotation class of knotted Legendrian tori in $\mathbb{R}^5$", *Topology Appl.* **209** (2016), 91–114. MR Zbl

[5] H. Brunn, "Über verknotete Kurven", pp. 256–259 in *Verhandlungen des ersten internationalen Mathematiker-Kongresses* (Zurich, 1897), 1897. Zbl

[6] S. Chang, "On Hamiltonian stable minimal Lagrangian surfaces in $\mathbf{C}\mathrm{P}^2$", *J. Geom. Anal.* **10**:2 (2000), 243–255. MR Zbl

[7] P. R. Cromwell, "Embedding knots and links in an open book, I: Basic properties", *Topology Appl.* **64**:1 (1995), 37–58. MR Zbl

[8] T. Ekholm, J. Etnyre, and M. Sullivan, "The contact homology of Legendrian submanifolds in $\mathbb{R}^{2n+1}$", *J. Differential Geom.* **71**:2 (2005), 177–305. MR Zbl

[9] T. Ekholm, J. Etnyre, and M. Sullivan, "Non-isotopic Legendrian submanifolds in $\mathbb{R}^{2n+1}$", *J. Differential Geom.* **71**:1 (2005), 85–128. MR Zbl

[10] T. Ekholm, J. Etnyre, and M. Sullivan, "Legendrian contact homology in $P \times \mathbb{R}$", *Trans. Amer. Math. Soc.* **359**:7 (2007), 3301–3335. MR Zbl

[11] T. Ekholm, L. Ng, and V. Shende, "A complete knot invariant from contact homology", 2016. Zbl arXiv 1606.07050

[12] P. Griffiths and J. Harris, *Principles of algebraic geometry*, Wiley-Interscience, New York, 1978. MR Zbl

[13] R. Harvey and H. B. Lawson, Jr., "Calibrated geometries", *Acta Math.* **148** (1982), 47–157. MR Zbl

[14] M. Haskins, "Special Lagrangian cones", *Amer. J. Math.* **126**:4 (2004), 845–871. MR Zbl

[15] H. Iriyeh, "Hamiltonian minimal Lagrangian cones in $\mathbf{C}^m$", *Tokyo J. Math.* **28**:1 (2005), 91–107. MR Zbl

[16] P. Lambert-Cole, "Legendrian Products", 2013. arXiv 1301.3700

[17] P. Lambert-Cole, *Invariants of Legendrian products*, Ph.D. thesis, Louisiana State University, 2014, available at https://digitalcommons.lsu.edu/gradschool_dissertations/2909/.

[18] H. Ma and Y. Ohnita, "Differential geometry of Lagrangian submanifolds and Hamiltonian variational problems", pp. 115–134 in *Harmonic maps and differential geometry*, Contemp. Math. **542**, Amer. Math. Soc., Providence, RI, 2011. MR Zbl

[19] L. L. Ng, "Computable Legendrian invariants", *Topology* **42**:1 (2003), 55–82. MR Zbl

[20] L. Ng, "Knot and braid invariants from contact homology: I", *Geom. Topol.* **9** (2005), 247–297. MR Zbl

[21] L. Ng, "Knot and braid invariants from contact homology: II", *Geom. Topol.* **9** (2005), 1603–1637. MR Zbl

[22] L. Ng, "Framed knot contact homology", *Duke Math. J.* **141**:2 (2008), 365–406. MR Zbl

[23] L. Ng and D. Thurston, "Grid diagrams, braids, and contact geometry", pp. 120–136 in *Proceedings of Gökova Geometry–Topology Conference* 2008, Gökova Geometry/Topology Conference (GGT), Gökova, 2009. MR Zbl

[24] Y.-G. Oh, "Second variation and stabilities of minimal Lagrangian submanifolds in Kähler manifolds", *Invent. Math.* **101**:2 (1990), 501–519. MR Zbl

[25] Y.-G. Oh, "Tight Lagrangian submanifolds in $\mathbf{CP}^n$", *Math. Z.* **207**:3 (1991), 409–416. MR Zbl

[26] Y.-G. Oh, "Volume minimization of Lagrangian submanifolds under Hamiltonian deformations", *Math. Z.* **212**:2 (1993), 175–192. MR Zbl

[27] H. Ono, "Hamiltonian stability of Lagrangian tori in toric Kähler manifolds", *Ann. Global Anal. Geom.* **31**:4 (2007), 329–343. MR Zbl

[28] P. Ozsvath, Z. Szabo, and D. Thurston, "Legendrian knots, transverse knots and combinatorial Floer homology", 2008. Zbl arXiv math/0611841v2

[29] J. Pati, "Contact homology of S^1-bundles over some symplectically reduced orbifolds", 2009. arXiv 0910.5934

[30] J. M. Sabloff, "Invariants of Legendrian knots in circle bundles", *Commun. Contemp. Math.* **5**:4 (2003), 569–627. MR Zbl

[31] R. Schoen and J. Wolfson, "Minimizing area among Lagrangian surfaces: the mapping problem", *J. Differential Geom.* **58**:1 (2001), 1–86. MR Zbl

[32] A. Strominger, S.-T. Yau, and E. Zaslow, "Mirror symmetry is T-duality", *Nuclear Phys. B* **479**:1-2 (1996), 243–259. MR Zbl

[33] F. Urbano, "Index of Lagrangian submanifolds of $\mathbf{C}\mathbf{P}^n$ and the Laplacian of 1-forms", *Geom. Dedicata* **48**:3 (1993), 309–318. MR Zbl

[34] J. Wolfson, "Two applications of prequantization in Lagrangian topology", *Pacific J. Math.* **215**:2 (2004), 393–398. MR Zbl

Received 31 Jan 2021. Revised 11 Nov 2021.

SCOTT BALDRIDGE: sbaldrid@math.lsu.edu
Department of Mathematics, Louisiana State University, Baton Rouge, LA, United States

BEN MCCARTY: ben.mccarty@memphis.edu
Department of Mathematical Sciences, University of Memphis, Memphis, TN, United States

DAVID VELA-VICK: shea@math.lsu.edu
Department of Mathematics, Louisiana State University, Baton Rouge, LA, United States

Volume Editors:

John A. Baldwin
Boston College
Boston, MA
United States

Hans U. Boden
McMaster University
Hamilton, ON
Canada

John B. Etnyre
Georgia Institute of Technology
Atlanta, GA
United States

Liam Watson
University of British Columbia
Vancouver, BC
Canada

The cover image is based on an illustration from the article "Khovanov homology and strong inversions", by Artem Kotelskiy, Liam Watson and Claudius Zibrowius (see p. 232).

Electronic copies can be obtained free of charge from http://msp.org/obs/5 and printed copies can be ordered from MSP (contact@msp.org).

The Open Book Series is a trademark of Mathematical Sciences Publishers.

ISSN: 2329-9061 (print), 2329-907X (electronic)

ISBN: 978-1-935107-11-8 (print), 978-1-935107-10-1 (electronic)

First published 2022.

MATHEMATICAL SCIENCES PUBLISHERS
798 Evans Hall #3840, c/o University of California, Berkeley CA 94720-3840
contact@msp.org **https://msp.org**

THE OPEN BOOK SERIES 5

Gauge Theory and Low-Dimensional Topology: Progress and Interaction

This volume is a proceedings of the 2020 BIRS workshop *Interactions of gauge theory with contact and symplectic topology in dimensions 3 and 4*. This was the 6th iteration of a recurring workshop held in Banff. Regrettably, the workshop was not held onsite but was instead an online (Zoom) gathering as a result of the Covid-19 pandemic. However, one benefit of the online format was that the participant list could be expanded beyond the usual strict limit of 42 individuals. It seemed to be also fitting, given the altered circumstances and larger than usual list of participants, to take the opportunity to put together a conference proceedings.

The result is this volume, which features papers showcasing research from participants at the 6th (or earlier) *Interactions* workshops. As the title suggests, the emphasis is on research in gauge theory, contact and symplectic topology, and in low-dimensional topology. The volume contains 16 refereed papers, and it is representative of the many excellent talks and fascinating results presented at the Interactions workshops over the years since its inception in 2007.

TABLE OF CONTENTS